

# Water Resources Research<sup>®</sup>

## RESEARCH ARTICLE

10.1029/2021WR029931

### Key Points:

- Collated depth profiles of subsurface water chemistry and stream chemistry provide direct data support for the shallow and deep hypothesis
- Stream chemistry at high and low discharge can be used to approximate shallow soil water and deep groundwater chemistry, respectively
- The shallow-versus-deep concentration contrast ( $C_{ratio}$ ) can predict the concentration-discharge (CQ) power law slope ( $b$ )

### Supporting Information:

Supporting Information may be found in the online version of this article.

### Correspondence to:











B. Stewart and L. Li,  
[bjs5781@psu.edu](mailto:bjs5781@psu.edu);  
[lili@engr.psu.edu](mailto:lili@engr.psu.edu)

### Citation:

Stewart, B., Shanley, J. B., Kirchner, J. W., Norris, D., Adler, T., Bristol, C., et al. (2022). Streams as mirrors: Reading subsurface water chemistry from stream chemistry. *Water Resources Research*, 58, e2021WR029931. <https://doi.org/10.1029/2021WR029931>

Received 4 MAR 2021  
 Accepted 19 OCT 2021

## Streams as Mirrors: Reading Subsurface Water Chemistry From Stream Chemistry

Bryn Stewart<sup>1</sup> , James B. Shanley<sup>2</sup> , James W. Kirchner<sup>3,4,5</sup> , David Norris<sup>6</sup> , Thomas Adler<sup>7</sup>, Caitlin Bristol<sup>7</sup>, Adrian A. Harpold<sup>8</sup> , Julia N. Perdrial<sup>7</sup> , Donna M. Rizzo<sup>9</sup> , Gary Sterle<sup>8</sup>, Kristen L. Underwood<sup>9</sup> , Hang Wen<sup>10</sup> , and Li Li<sup>1</sup> 

<sup>1</sup>Department of Civil and Environmental Engineering, The Pennsylvania State University, University Park, PA, USA, <sup>2</sup>U.S. Geological Survey, New England Water Science Center, USGS, Montpelier, VT, USA, <sup>3</sup>Department of Environmental Systems Science, ETH Zürich, Zürich, Switzerland, <sup>4</sup>Swiss Federal Research Institute WSL, Birmensdorf, Switzerland, <sup>5</sup>Department of Earth and Planetary Science, University of California, Berkeley, CA, USA, <sup>6</sup>UK Centre for Ecology and Hydrology, Environment Centre Wales, Bangor, UK, <sup>7</sup>Department of Geology, University of Vermont, Burlington, VT, USA, <sup>8</sup>Department of Natural Resources and Environmental Science, University of Nevada, Reno, NV, USA, <sup>9</sup>Department of Civil and Environmental Engineering, University of Vermont, Burlington, VT, USA, <sup>10</sup>School of Earth System Science, Tianjin University, Tianjin, China

**Abstract** The shallow and deep hypothesis suggests that stream concentration-discharge (CQ) relationships are shaped by distinct source waters from different depths. Under this hypothesis, baseflows are typically dominated by groundwater and mostly reflect groundwater chemistry, whereas high flows are typically dominated by shallow soil water and mostly reflect soil water chemistry. Aspects of this hypothesis draw on applications like end member mixing analyses and hydrograph separation, yet direct data support for the hypothesis remains scarce. This work tests the shallow and deep hypothesis using co-located measurements of soil water, groundwater, and streamwater chemistry at two intensively monitored sites, the W-9 catchment at Sleepers River (Vermont, United States) and the Hafren catchment at Plynlimon (Wales). At both sites, depth profiles of subsurface water chemistry and stream CQ relationships for the 10 solutes analyzed are broadly consistent with the hypothesis. Solute that are more abundant at depth (e.g., calcium) exhibit dilution patterns (concentration decreases with increasing discharge). Conversely, solutes enriched in shallow soils (e.g., nitrate) generally exhibit flushing patterns (concentration increases with increasing discharge). The hypothesis may hold broadly true for catchments that share such biogeochemical stratifications in the subsurface. Soil water and groundwater chemistries were estimated from high- and low-flow stream chemistries with average relative errors ranging from 24% to 82%. This indicates that streams mirror subsurface waters: stream chemistry can be used to infer scarcely measured subsurface water chemistry, especially where there are distinct shallow and deep end members.

## 1. Introduction

Streams and rivers collect waters from shallow soils, regolith, and bedrock in the subsurface. Subsurface chemical structure and physical characteristics vary considerably with depth as climate, vegetation, and rocks interact over geological time scales (Brantley et al., 2017; Li et al., 2017; Riebe et al., 2017). When meteoric water infiltrates and solubilizes rocks, pores open up such that greater permeability generally develops in the near-surface shallow soils than at depth (Welch & Allen, 2014). Shallow soils therefore typically contain more weathered materials enriched with clays, whereas the deeper subsurface harbors more actively weathering parent rocks (Jin et al., 2010; McIntosh et al., 2017). Shallow soils also have abundant organic materials and nutrients that are signatures of life (Barnes et al., 2018; Jobbágy & Jackson, 2000; Pinay et al., 2015). Soil biogeochemical processes, such as the deposition and decomposition of organic matter, drive carbon and nutrient cycling and regulate their concentration profiles in the subsurface. In contrast to shallow soils, the deeper subsurface often has less labile organic matter. These biogeochemical and hydrological stratifications collectively regulate water flow paths and the contact times between water, biota, soils, and rocks, thereby governing reaction rates and water chemistries in soils, groundwater, and streams. Broadly, these water chemistries are important measures of water quality (Worrall et al., 2008). They also reflect the rates of biogeochemical reactions and the response of the Earth's surface and subsurface to changing climate and human perturbations (Li et al., 2021).

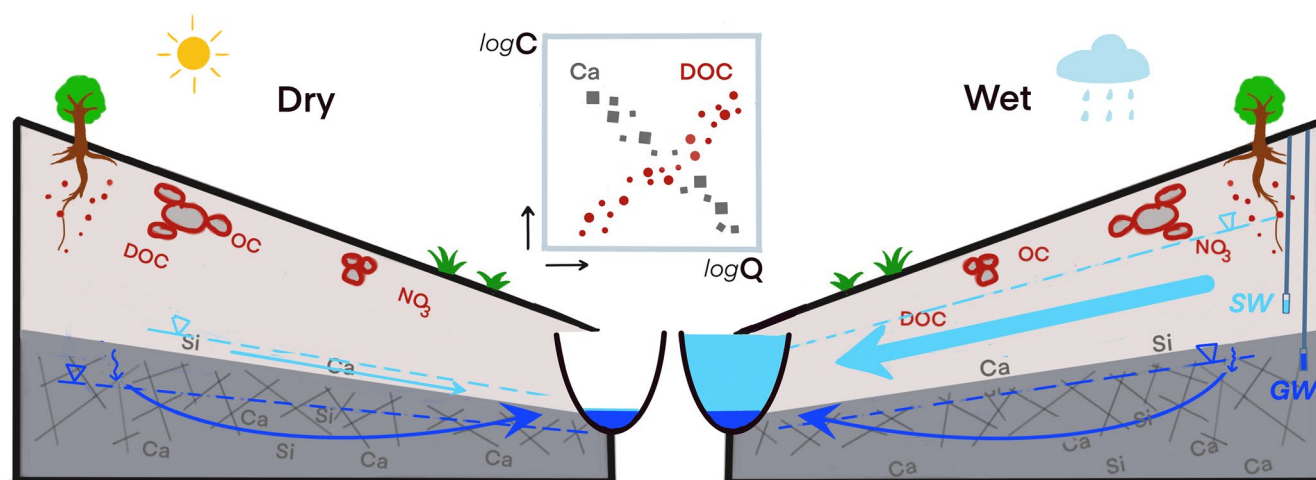


**Figure 1.** A conceptual figure illustrating shallow and deep water flows under different hydrological conditions. “SW” refers to soil water (shallow water), and “GW” refers to groundwater (deep water). The left hillslope is under “dry” or low-flow conditions when groundwater mostly supplies baseflow. The right hillslope is under “wet” or high-flow conditions when more water flows through shallow soils. The shallow and deep hypothesis holds that the distinct chemistry of shallow and deep waters is reflected in concentration-discharge (CQ) patterns, with deep waters dominating stream chemistry under low-flow conditions (left) and shallow waters dominating stream chemistry under high-flow conditions (right). This theory is illustrated in the figure with two representative solutes, calcium (Ca) and dissolved organic carbon (DOC), where Ca has higher concentrations in deep waters and low streamflows, while DOC has higher concentrations in shallow waters and high streamflows.

The hydrology community has long recognized that streamwater is a mixture of source waters from distinct flow paths at different depths (Boyer et al., 1997; Klaus & McDonnell, 2013; Neal et al., 2012; Pinder & Jones, 1969). Under low-flow conditions, deeper flow paths sustain streamflow, especially during extended dry-weather and warm conditions (Haria & Shand, 2004; McGlynn et al., 2002; Tallaksen, 1995; Wittenberg, 1999). Under wet conditions (e.g., snowmelt, storms), hydraulic conductivity increases toward the land surface as water saturation increases (Laudon et al., 2004). Such conditions often lead to higher infiltration, rising water tables, and high flows via shallow, permeable soils (Bishop et al., 2004; Pacific et al., 2010; Seibert et al., 2009), which contribute to the predominance of young, shallow soil water in streams (Berghuijs & Kirchner, 2017; Dunne & Black, 1971; Jasechko et al., 2016; Mulholland, 1993).

The shallow and deep flow paths carry distinct water chemistry that is regulated by subsurface hydro-bio-geochemical structure and water transit times. Groundwater from deeper zones typically has a longer transit time (Frisbee et al., 2013) and is more enriched with base cations than shallow water (Anderson et al., 1997). In contrast, younger water chemistry in shallow soils is typically more enriched with organic materials (Neal et al., 2012; Sullivan et al., 2016; Torres et al., 2015). At Plynlimon in Wales, streamwater chemistry transitions from an acidic soil water signature during storms to a base-rich, alkaline groundwater signature at low flows (Neal et al., 1990; Shand et al., 2005). At Sleepers River in Vermont, streamwater shifts between a soil water signature with high dissolved organic carbon (DOC) and nitrate ( $\text{NO}_3$ ) at high flows to a cation- and carbonate-rich groundwater signature at low flows (Kendall et al., 1999).

These observations lead to the shallow and deep hypothesis (Zhi & Li, 2020; Zhi et al., 2019) that stream chemistry is determined by the chemistries of source waters from two predominantly contributing flow paths, one via shallow soils and another via deeper regolith and fractured bedrock; the chemical contrasts between the two source waters shape solute export patterns, or the power-law slope ( $b$ ) of the concentration-discharge (CQ) relationship ( $C = aQ^b$ ) (Figure 1). Although not explicitly called the shallow and deep hypothesis, this idea has long been explored in the hydrology and biogeochemistry communities. The concepts of distinct source waters and flow paths have been used in hydrograph separation (Pinder & Jones, 1969) and End Member Mixing Analysis (EMMA) to infer contributions of different waters to streams under different hydrological conditions (Evans & Davies, 1998; Hooper et al., 1990; Johnson et al., 1969; Klaus & McDonnell, 2013). Solute export patterns have also been linked to spatial heterogeneity of source areas and flow generation zones (Basu et al., 2010; Musolff

et al., 2016, 2017) as well as reaction rates and conductivity profiles in the subsurface (Ameli et al., 2017; Wen & Li, 2018).

Recent studies have further underscored the importance of shallow and deep water chemical contrasts in explaining CQ relationships (Godsey et al., 2009, 2019; Thompson et al., 2011). The Riparian Profile Flow-Integration Model (RIM) quantitatively linked the vertical profiles of riparian water chemistry and fluxes at different depths to solute export patterns in streams (Seibert et al., 2009). Higher permeability contrasts in shallow and deep subsurface have been shown to amplify the contrasts between soil water and groundwater chemistry, therefore leading to more dilution CQ patterns for weathering products (Xiao et al., 2021). Solute export patterns, quantified by the power-law slope ( $b$ ) value in the CQ relationship ( $C = aQ^b$ ), often correlate with the ratios of solute concentrations in shallow and deep waters ( $C_{\text{ratio}}$ ). This correlation was confirmed for 13 solutes at three catchments and in 500 Monte Carlo simulations (Zhi et al., 2019). The relationship between  $b$  and  $C_{\text{ratio}}$  (with different parameter values) has been shown to describe the export patterns of  $\text{NO}_3$  in more than 200 watersheds spanning a range of climate, geology, and land use conditions in the United States (Zhi & Li, 2020). Vertical solute distribution predominantly shapes  $\text{NO}_3$  export patterns in 278 catchments in Germany (Ebeling et al., 2021). A global scale analysis examining multiple solutes and their controlling factors further supports the idea that the depth of solute generation is a stronger determinant of CQ slope than climatic drivers are (Botter et al., 2020).

Despite widespread recognition of the shallow and deep hypothesis, direct data support of the hypothesis using measured stream chemistry in conjunction with subsurface water chemistry at different depths is rare. Although subsurface data have become more available in recent years (Brantley et al., 2007), very few sites have co-located, comprehensive soil water, groundwater, and stream chemistry data. Soil water sampling requires the installation of lysimeters, while deeper groundwater sampling typically demands expensive and labor-intensive borehole drilling. While previous works (Zhi & Li, 2020; Zhi et al., 2019) have used watershed reactive transport modeling to link modeled subsurface water chemistry with stream chemistry, the lack of co-measured stream and subsurface water chemistry limited the direct validation of the shallow and deep hypothesis.

Here we test the hypothesis using co-located solute chemistry data from streams, soil waters, and groundwaters at two intensively monitored catchments, the W-9 catchment in the Sleepers River Research Watershed (SRRW) in Vermont, United States, and the Hafren catchment at Plynlimon in Wales, United Kingdom. If the shallow and deep hypothesis is true, measured stream chemistry under different flow conditions is expected to approximate measured subsurface water chemistry and stratification. Namely, (a) Solute depth profiles shape their CQ relationship: solutes that are abundant in deep waters but relatively depleted in shallow waters exhibit a dilution CQ pattern, with high stream concentrations at low flow and low stream concentrations at high flow; solutes that are scarcely present in deep waters but enriched in shallow waters exhibit a flushing CQ pattern, with low stream concentrations at low flow and high stream concentrations at high flow; (b) Stream chemistry under low- and high-flow conditions can approximate groundwater and soil water chemistry, respectively; (c) The CQ power law slope ( $b$ ) values correlate with the shallow-versus-deep concentration ratio ( $C_{\text{ratio}}$ ) as supported by the shallow and deep hypothesis.

## 2. Methodology

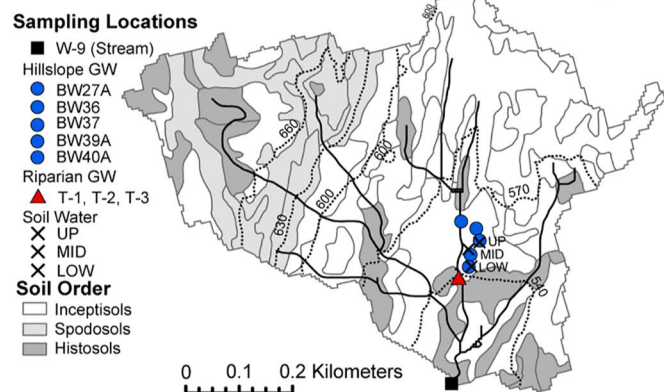
### 2.1. Site Descriptions

#### 2.1.1. W-9 Catchment, Sleepers River, VT

The W-9 catchment at the SRRW in northeastern Vermont has a drainage area of 0.405 km<sup>2</sup> and is entirely forested. Elevation ranges from 524 to 679 m with slopes from 0% to 90% (Kendall et al., 1999). The SRRW has a humid continental climate with a mean annual precipitation of 1320 mm (Armfield et al., 2019). Approximately 60% of precipitation leaves the catchment via stream runoff while evapotranspiration accounts for the remaining 40%. Snowfall typically accounts for 20%–30% of annual precipitation (Shanley, 2000).

Soils in the W-9 catchment (Figure 2a) are heterogeneous, ranging from poorly drained histosols in riparian areas to well-drained inceptisols and spodosols on hillslopes (DeKett & Long, 1995; Shanley et al., 2004). Beneath the

(a) W-9 Catchment,  
Sleepers River, Vermont,  
United States



(b) Hafren Catchment,  
Plynlimon, Wales,  
United Kingdom

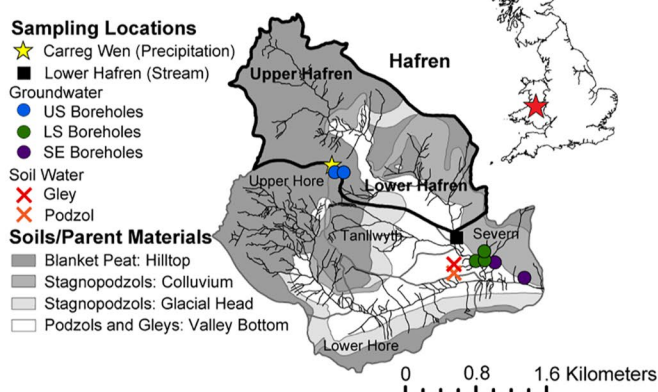


**Figure 2.** (a) Soil map of the W-9 catchment (0.405 km<sup>2</sup>) at Sleepers River Research Watershed with sampling locations. Elevation contours (dotted lines) in meters. Details of each soil type are from DeKett and Long (1995). (b) Map of the Hafren catchment (4.8 km<sup>2</sup>) at Plynlimon. The map includes sub-catchment boundaries, sampling locations, and general distribution of soils/parent materials. Groups of groundwater boreholes are distinguished by color and abbreviated as follows: Upper Slope (US), Lower Slope (LS), and South East (SE). Details of soils and parent materials from Bell (2005) and Brandt et al. (2004). Note that soil types/orders correspond to U.S. and U.K. terminology by catchment (e.g., “spodosols” in the United States are equivalent to “podzols” in the United Kingdom).

surficial soils lies a 1–4 m layer of glacial till, formed from the local quartz-mica schist and calcareous granulite bedrock. The presence of carbonate in the bedrock and till provides a high buffering capacity, which helped to neutralize acid deposition (Shanley, 2000). Riparian flow paths notably change from deep groundwater to displaced upslope water during the snowmelt period (Dunne & Black, 1971; McGlynn et al., 1999).

Riparian groundwater is the major source of streamflow in the early stages of snowmelt, while hillslope till and soil water contribute more during the later stages (Kendall et al., 1999). An end member mixing analysis (Kendall et al., 1999) has further suggested that the two dominant sources of streamwater are riparian groundwater (via deep flow paths) and soil water (via shallow flow paths). Groundwater typically dominates the hydrograph, though stream chemistry during storm and snowmelt events reflects the chemical signature of surficial soil water (Shanley et al., 2002, 2015). Distinct chemical contrasts exist between the surficial soils, glacial till, and underlying bedrock, partly due to the varying extent of weathering and different abundance of minerals and organic matter. Each subsurface layer thus has a unique chemical signature.

The temporal dynamics of discharge, precipitation, and air temperature at the W-9 catchment for 2009 (Figure 3a) are representative of temperate climates that are seasonally snow-dominated. Snowpack accumulates throughout

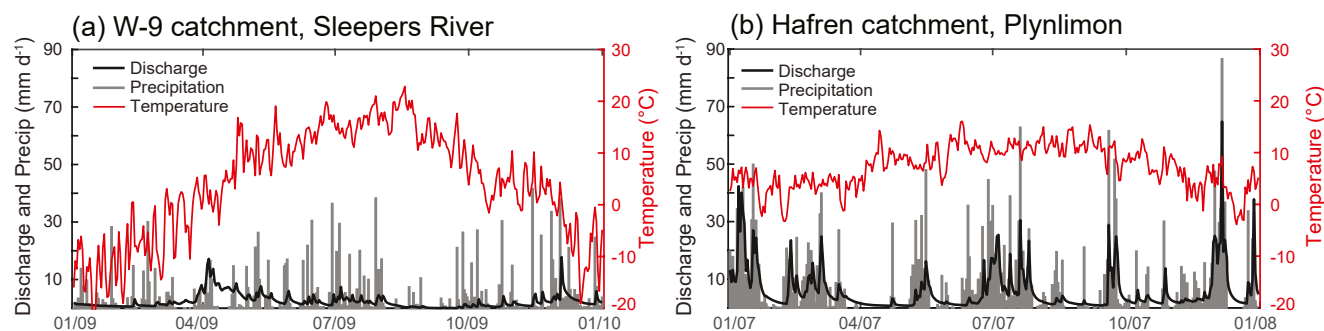


**Figure 3.** (a) Daily time series of discharge, precipitation, and air temperature in 2009 for the W-9 catchment at Sleepers River, Vermont (Shanley et al., 2021). The runoff ratio (mean discharge/mean precipitation) is 0.65. (b) Daily time series of discharge, precipitation, and air temperature in 2007 for the Hafren catchment at Plynlimon, Wales. The runoff ratio is 0.78. The temporal dynamics demonstrate the climatic similarities and differences between the two sites.



the winter, as shown by peaks in precipitation but relatively constant and low discharge from January to March. The major hydrological event is snowmelt, typically occurring in early April and accounting for up to 50% of annual streamflow (Shanley, 2000). Precipitation occurs throughout the year, though low streamflows are consistently observed from August to September, as the bulk of rainfall is apportioned to evapotranspiration during these months. Despite this, baseflows are sustained by the high storage capacity of glacial till in the subsurface (Shanley et al., 2015).

### 2.1.2. Hafren Catchment, Plynlimon, Wales

The Plynlimon research catchments (Figure 2b) are located in central Wales and include the headwaters of the River Severn and River Wye. The catchments are about 20 km away from the sea, which provides a temperate, maritime climate, and the influence of sea spray and aerosols (Neal & Kirchner, 2000). Elevation ranges from 340 to 740 m, and mean annual precipitation is 2500 mm (Reynolds et al., 1997). The Hafren catchment (4.8 km<sup>2</sup>) contains the headwaters to the River Severn and comprises the Upper Hafren and Lower Hafren sub-catchments. The Upper Hafren is 1.22 km<sup>2</sup> of shrubland and bog used for low-intensity sheep grazing, and is characterized by poorly drained, acidic peat soils (Kirby et al., 1991). The Lower Hafren is 3.58 km<sup>2</sup> of coniferous plantation forest, dominated by Sitka spruce, developed on a mixture of peaty gley and stagnopodzol soils (Bell, 2005; Brandt et al., 2004). The entire catchment is underlain by sandstone, mudstone, and shale bedrock (Neal et al., 1990; Reynolds et al., 1988).

Shallow bedrock is highly fractured throughout the catchment, creating hydrological pathways and areas of water storage. Bedrock groundwater is heterogeneous, with chemical stratification due to different flow paths and groundwater compartments (Haria & Shand, 2004). Shallow soil waters and deep groundwaters are not well connected, but vertical mixing may occur (Shand et al., 2007). Tracer data from Plynlimon imply that the hillslopes store and release water over a wide range of time scales, with extensive mixing resulting from subsurface heterogeneity (Kirchner & Neal, 2013; Kirchner et al., 2000, 2001; Knapp et al., 2019).

The time series of discharge, precipitation, and air temperature at the Lower Hafren catchment (Figure 3b) exhibits only weak seasonality in precipitation. Unlike the W-9 catchment at SRRW, the temperature in the Hafren catchment does not vary as much. Hafren does not have an extended low-flow period during the summer, though low-flow conditions are observed sporadically. High-flow conditions typically occur in response to precipitation events, and no snowmelt signature is present.

## 2.2. Data Summary

### 2.2.1. W-9, Sleepers River

The W-9 catchment at Sleepers River has rich hydrologic and chemical data (Table S1 in Supporting Information S1; sampling locations in Figure 2a). We used stream discharge data along with chemistry data for the stream, precipitation, groundwater, and soil water (Matt et al., 2021). Groundwater chemistry was measured in the hillslope ("BW-" wells) and the riparian area ("T-" wells, which are nested piezometers) (Shanley et al., 2019). Soil water chemistry was determined from zero-tension lysimeters at three locations (Figure 2a) co-located with three of the hillslope wells, where the UP, MID, and LOW slope lysimeters correspond to the BW39A, BW40A, and BW27A hillslope wells, respectively. As zero-tension lysimeters primarily sample water from soil macropores, the soil water chemistry should represent the shallow water that can be mobilized to the stream (Swistock et al., 1990). The major chemical species analyzed for all source waters include: pH, acid neutralizing capacity (ANC), calcium (Ca), chloride (Cl), DOC, potassium (K), magnesium (Mg), sodium (Na), NO<sub>3</sub>, silicon (Si), and sulfate (SO<sub>4</sub>).

### 2.2.2. Hafren, Plynlimon

We used long-term stream and precipitation chemistry data from the Lower Hafren catchment (Neal et al., 2013; Norris et al., 2017, 2019) (Table S2 in Supporting Information S1; sampling locations in Figure 2b). Groundwater chemistry samples were collected from boreholes at multiple locations (Neal et al., 2013; Shand et al., 2005). Soil water samples were collected by zero-tension lysimeters and ceramic suction cup samplers for four horizons at two pits (Figure 2b). Each pit represents a major soil, including

podzols and gleys. The podzol and gley soil water samples were collected near the Lower Hafren flume and represent the Lower Hafren catchment (Herndon et al., 2015; Shand et al., 2005; Stevens et al., 1997). While over 40 chemical species were measured for the streamwater at the Hafren catchment, records are limited for soil water and groundwater chemistry. The major chemical species analyzed in all source waters include: pH, Gran alkalinity, aluminum (Al), Ca, Cl, DOC, iron (Fe), K, Mg, Na, NO<sub>3</sub>, Si, and SO<sub>4</sub>. However, Al and DOC were not measured for boreholes LS1-LS3 nor US1-US3. SO<sub>4</sub> measurements in streamwater from April 2012 to March 2013 were excluded from the analysis due to substantial differences from other measurements, indicating potential inaccuracies.

### 2.3. CQ Analysis

CQ relationships have been widely used to describe solute export patterns (Boyer et al., 1997; Diamond & Cohen, 2018; Godsey et al., 2009, 2019; Thompson et al., 2011). Various CQ characterization approaches have been proposed (Hoagland et al., 2017; Moatar et al., 2017; Musolff et al., 2015). Here we use the power-law relationship  $C = aQ^b$ , where  $C$  is concentration,  $Q$  is discharge, and  $a$  and  $b$  are fitted parameters. When concentration and discharge are plotted on a log-log scale, the resulting slope corresponds to the power-law slope value  $b$ . The three basic CQ patterns of flushing, constant, and dilution are generally reflected in values of the power-law slope ( $b$ ). We follow conventions in literature and define flushing (i.e., enrichment) patterns as those corresponding to values of  $b \geq 0.1$ , indicating that solute concentrations increase with increasing discharge, and dilution patterns as those corresponding to values of  $b \leq -0.1$ , where concentrations decrease with increasing discharge. Values of  $b$  between  $-0.1$  and  $0.1$  correspond to constant or flat patterns (Musolff et al., 2015, 2017; Thompson et al., 2011). Solutes may exhibit relatively stable trends in  $C$  compared to  $Q$ , otherwise known as chemostatic behavior. In contrast, solutes may also show substantial variability in  $C$  with changing  $Q$ , known as chemodynamic behavior (Musolff et al., 2015; Thompson et al., 2011). While the distinction between chemostatic and chemodynamic behavior is typically quantified by the ratio of coefficients of variation for concentration and discharge ( $CV_C/CV_Q$ ), we focus our analysis on  $b$  values. Values of  $b$  and  $CV_C/CV_Q$  ratios for each solute are listed in Table S3 in Supporting Information S1. Note that pH, ANC, and Gran alkalinity are not included in the  $b$  value calculations.

### 2.4. The Mixing Model and the Shallow and Deep Source Waters

Following Figure 1, streamflow ( $Q_{\text{stream}}$ ) is predominantly the sum of two end member source waters: the shallow soil water ( $Q_{\text{sw}}$ ) and deeper groundwater ( $Q_{\text{gw}}$ ). The two source waters carry distinct water chemistry represented by their respective solute concentrations ( $C_{\text{sw}}$  and  $C_{\text{gw}}$ ). Stream chemistry ( $C_{\text{stream}}$ ) is thus determined by both flow proportion of the two waters and their corresponding chemistry. The following equations can be formulated based on mass balance principles:

$$Q_{\text{stream}}(t) = Q_{\text{sw}}(t) + Q_{\text{gw}}(t) \quad (1)$$

$$C_{\text{stream}}(t)Q_{\text{stream}}(t) = C_{\text{sw}}(t)Q_{\text{sw}}(t) + C_{\text{gw}}(t)Q_{\text{gw}}(t) \quad (2)$$

Values of  $Q$  and  $C$  depend on time, as illustrated in Figure 4. Streamflow often changes by orders of magnitude; water chemistry does not change as much, especially in groundwater. Equation 2 can be simplified using averaged concentrations as representative chemistry of shallow and deeper zones:

$$C_{\text{stream}}(t)Q_{\text{stream}}(t) \equiv \overline{C_{\text{sw}}}Q_{\text{sw}}(t) + \overline{C_{\text{gw}}}Q_{\text{gw}}(t) \quad (3)$$

$$C_{\text{stream}}(t) \equiv \overline{C_{\text{sw}}} \frac{Q_{\text{sw}}(t)}{Q_{\text{stream}}(t)} + \overline{C_{\text{gw}}} \frac{Q_{\text{gw}}(t)}{Q_{\text{stream}}(t)} \quad (4)$$

Under wet conditions, shallow water often dominates in the stream ( $Q_{\text{sw}}(t) \gg Q_{\text{gw}}(t)$  and  $Q_{\text{sw}}(t) \approx Q_{\text{stream}}(t)$ ), such that  $C_{\text{stream}} \approx \overline{C_{\text{sw}}}$ ; under dry conditions, deeper groundwater dominates in the stream ( $Q_{\text{sw}}(t) \ll Q_{\text{gw}}(t)$  and  $Q_{\text{gw}}(t) \approx Q_{\text{stream}}(t)$ ), such that  $C_{\text{stream}} \approx \overline{C_{\text{gw}}}$ .

We can therefore use stream chemistry at high flow to estimate the average chemistry of soil water, and stream chemistry at low flow to approximate the average chemistry of groundwater (Figure 1). Similar formulations have been developed for hydrograph separation of pre-event versus event waters (see reviews in Buttle, 1994; Klaus & McDonnell, 2013). The equations here follow the idea of the shallow and deep hypothesis and assume minimal surface runoff, a common assumption in hydrograph separation. The estimated shallow and deep water chemistries represent the average chemistry in the shallow and deep zones that enter streams. They are not meant to represent the temporal and spatial variations in shallow and deep water chemistry.

## 2.5. Estimating Shallow Water (Soil Water) and Deep Water (Groundwater) Chemistry

To test whether the chemical compositions of groundwater and soil water could be inferred using stream chemistry data, we first compared daily discharges to discharges with corresponding chemistry measurements (“sampled discharges”) at each site. We removed samples of stream chemistry that were collected in addition to the weekly sampling at W-9 to remove bias toward high flows. We generated flow duration curves to confirm that the stream chemistry sampling at both sites was unbiased with respect to discharge (Figure S1 in Supporting Information S1) (Searcy, 1959). As it is uncertain at which flow range soil water becomes dominant, soil water chemistry was estimated as the average of the stream chemistry during the highest 1%, 2%, 5%, and 10% of sampled discharges. Similarly, the groundwater chemistry was estimated as the averages of the stream chemistry during the lowest 1%, 2%, 5%, and 10% of sampled discharges. These high-flow and low-flow chemistry estimates were compared to average measured concentrations in soil water and groundwater samples, respectively.

At W-9, riparian groundwater chemistry was calculated from the average chemistry of the nested piezometers (“T-” wells), and hillslope groundwater chemistry was averaged from hillslope wells (“BW-” wells); soil water chemistry was calculated from the average chemistry of all lysimeters. At Hafren, US groundwater chemistry was calculated from the average chemistry of the Upper Slope boreholes (US1, US2, and US3); the LS groundwater chemistry was averaged from the Lower Slope boreholes (LS1, LS2, LS3, and LS4); and the SE groundwater chemistry was averaged from the South East boreholes (SE1 and SE3). The podzol soil water chemistry was calculated from the average chemistry of all horizons in the podzol samples, and the gley soil water chemistry was averaged from all horizons in the gley samples.

To quantify the relative error  $\varepsilon$  of each solute estimate, we calculated

$$\varepsilon = \frac{\overline{C_E} - \overline{C_M}}{\overline{C_M}} \quad (5)$$

where  $\overline{C_E}$  is the mean estimated concentration and  $\overline{C_M}$  is the mean measured concentration. All relative error values are listed in Table S4 in Supporting Information S1. We used the following uncertainty propagation procedure to account for variability in the datasets. We first calculated the mean, standard deviation, and standard error for concentrations for each solute at each individual location (e.g., US1, US2, US3 boreholes). Next, we calculated the mean measured concentration,  $\overline{C_M}$ , for each sampling group (e.g., US GW) as the arithmetic average of the individual location means. To account for both the variability in individual locations and between sample locations (e.g., well-to-well), we calculated two uncertainty estimates. The first estimate was propagated from the standard errors of each sample location mean (accounting for variability in each location), and the second uncertainty estimate was derived from the standard deviation among the sample locations of each group (accounting for well-to-well and lysimeter-to-lysimeter differences in mean concentrations). These two standard error estimates were combined in quadrature to yield a conservative uncertainty estimate in which the larger component dominates (Table S5 in Supporting Information S1). Details are outlined in Text S2 in Supporting Information S1. The mean concentration values and corresponding standard error values calculated following this procedure are in Table S5 in Supporting Information S1. A seasonal analysis was performed by calculating mean concentrations from the soil water and groundwater chemistry data partitioned by seasons, defined as winter (January–March), spring (April–June), summer (July–September), and autumn (October–December). Seasonal estimates for subsurface chemistry were calculated from

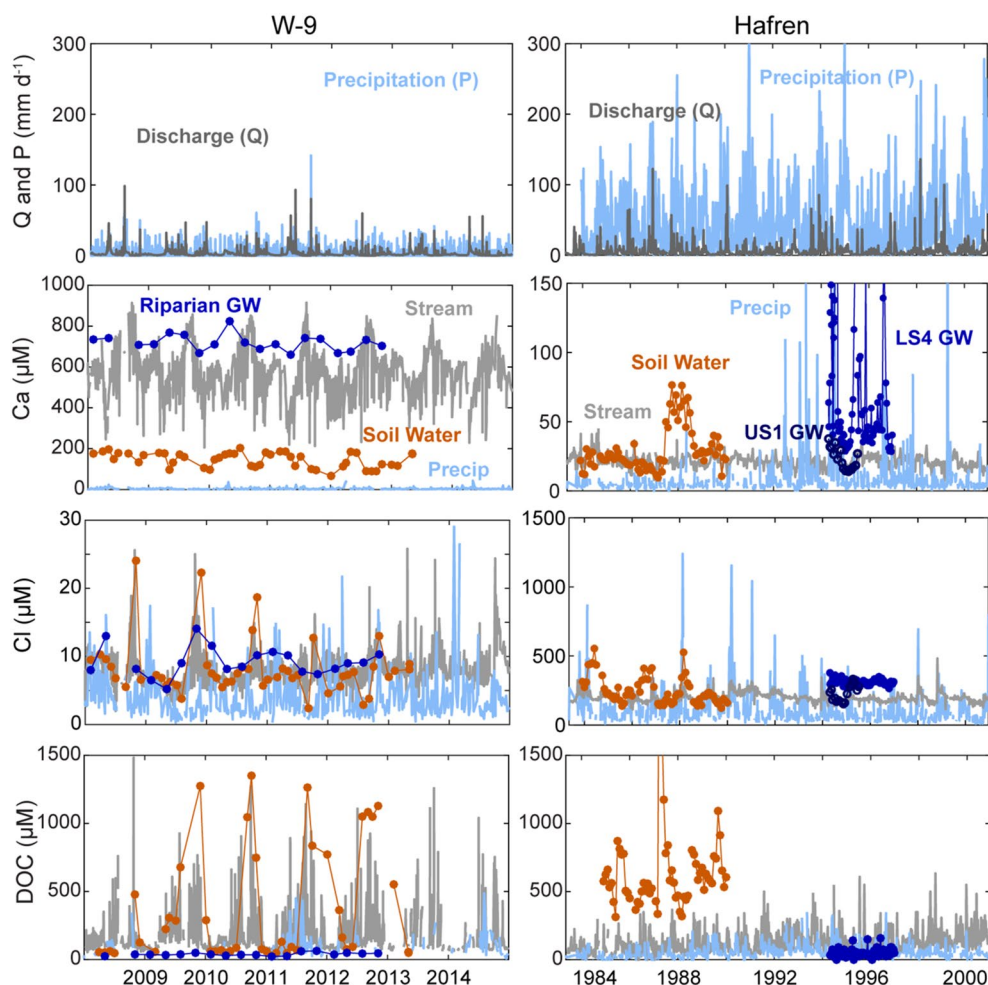


**Figure 4.** Time series of discharge, precipitation, and three representative solutes, Ca, Cl, and DOC, in different source waters at W-9, Sleepers River (left column) and Hafren, Plynlimon (right column). For W-9, soil water chemistry is from the LOW lysimeter and groundwater chemistry is from the deepest riparian piezometer (T-1). For Hafren, stream chemistry is from the Lower Hafren flume and soil chemistry is the monthly average of the E, C, and B horizons of the podzol samples; groundwater chemistry is shown for the LS4 and US1 boreholes (DOC was not measured for US1). Discharge and precipitation are in  $\text{mm d}^{-1}$ . Concentrations are in  $\mu\text{M}$ . These plots illustrate how different solutes are enriched in different source waters and how stream chemistry reflects a mixture of those sources.

stream chemistry partitioned by seasons and by flow conditions within each season. This approach did not lead to more accurate analysis.

These simple approaches are intended to provide first-order estimates for subsurface water chemistry before more complicated and rigorous approaches (e.g., EMMA) are used, or in situations where other approaches cannot be applied. We anticipated disparity between measured and estimated chemistry values, as deeper groundwater is never entirely absent at any range of the hydrograph at either site. More specifically, at Sleepers River, groundwater isotopic signatures have been found to be present even during snowmelt (McGlynn et al., 1999). Similarly, at Plynlimon, water from the deeper subsurface contributes a significant portion of the total streamflow (25%–50%) even at high flow (Neal et al., 1990). In addition, precipitation contributes to both soil water and groundwater via infiltration and recharge, meaning that precipitation chemistry influences the chemical signatures of subsurface waters. For this reason, we consider the soil water and groundwater chemistries to integrate the contribution of precipitation and do not include a separate end member for precipitation.



### 3. Results

#### 3.1. Temporal Variation of Solute Concentrations in Different Waters

The concentrations of three representative solutes (Ca, Cl, and DOC) in precipitation, streamwater, soil water, and groundwater show large temporal variations in both catchments (Figure 4). Ca concentrations are highest in groundwater at both catchments, but are much higher at W-9 due to the calcareous till and bedrock. Ca concentrations are generally lowest in precipitation. Streamwater concentrations fall in between soil water and groundwater and vary inversely to stream discharge. This indicates that streamwater mostly comes from soil water and groundwater with a negligible contribution directly from the precipitation water. Cl has relatively similar concentrations in shallow (soil water) and deep (groundwater) waters at both catchments. At Hafren, peaks of stream Cl coincide with those in precipitation but are strongly damped; this indicates that Cl from precipitation is not transported immediately to the stream, even though Cl is primarily from atmospheric deposition (Kirchner et al., 2000; Neal & Rosier, 1990). For both catchments, DOC concentrations are highest in the soil water and lowest in groundwater. Soil water DOC has significant variations across seasons. Similar to Ca, stream DOC concentrations fall between soil water and groundwater concentrations, indicating the contribution of these waters to streamflow.

#### 3.2. Solute Depth Profiles and CQ Plots

Although both catchments have measurements for additional chemical species, the solutes in Figure 5 are those with samples in streamwater, groundwater, and soil water. These solutes exhibit dilution, constant, and flushing CQ patterns. Solute that are abundant at depth exhibit dilution patterns (e.g., Ca, Mg, and Si) with highest stream concentrations at low flows and lowest stream concentrations at high flows. Comparing the depth profiles with corresponding CQ figures indicates that the highest stream concentrations are generally within the range of the concentrations in the deeper subsurface (below 2 m). For example, the highest concentrations of Ca occur at low discharge for both sites, approximating 600–800  $\mu\text{M}$  at W-9 and 40–60  $\mu\text{M}$  at Hafren. These values are similar to the deeper groundwater concentrations in the depth profiles. The lowest Ca concentrations occur at high discharge in both sites, approximating 25–200  $\mu\text{M}$  at W-9 and 10–20  $\mu\text{M}$  at Hafren. These concentrations are within the range of shallow soil water concentrations for each site.

Chloride is the only solute with  $b$  values close to zero at both sites. The small  $b$  values arise from variations in concentration but no systematic trend with discharge. Cl is primarily derived from atmospheric deposition. It is generally non-reactive and only weakly sorbing, which leads to no preferential retention. However, Cl can precipitate out during dry times of the year. Cl has negligible vertical stratification in the depth profiles. In addition, Cl concentrations vary substantially between the two sites. At W-9, Cl concentrations vary from 7 to 14  $\mu\text{M}$ ; at Hafren, they vary between 200 and 300  $\mu\text{M}$ . The much higher Cl concentrations at Hafren are due to the site's close proximity to the ocean.

In both catchments, DOC and  $\text{NO}_3$  exhibit flushing patterns. Their concentrations are higher in the shallow soils than in the deeper subsurface, although the difference is more pronounced for DOC. At W-9, the lowest stream DOC concentrations occur at intermediate discharge and are 30–50  $\mu\text{M}$ , corresponding to DOC concentrations in the deeper groundwater. At the lowest discharge, stream DOC concentrations approximate 100  $\mu\text{M}$ . Separating the CQ data for DOC by season shows that the lowest concentrations at intermediate discharge occur in winter and spring whereas the intermediate concentrations occur at lowest flows in summer (Figure S2 in Supporting Information S1). DOC concentrations increase significantly at high discharge, approaching 1000–1500  $\mu\text{M}$ . At Hafren, DOC concentrations increase from around 20–100  $\mu\text{M}$  to peak values around 1000  $\mu\text{M}$ . At W-9,  $\text{NO}_3$  concentrations are typically 7–10  $\mu\text{M}$  at low discharge, but range from 0.1 to 30  $\mu\text{M}$  at intermediate discharge.  $\text{NO}_3$  shows an increasing trend with discharge similar to DOC, only weaker, with concentrations ranging from 1 to 50  $\mu\text{M}$  at high discharge. At Hafren,  $\text{NO}_3$  concentrations (1–20  $\mu\text{M}$ ) are lowest at low discharge and generally increase with discharge.

Sulfate shows different CQ patterns between the two sites. At W-9,  $\text{SO}_4$  exhibits a dilution pattern with maxima around 100  $\mu\text{M}$  at low discharge and decreases as discharge increases, reaching minima around 20  $\mu\text{M}$ . This pattern is consistent with  $\text{SO}_4$  concentration increasing with depth. At Hafren,  $\text{SO}_4$  exhibits no systematic response to discharge variation with visible scatter at high discharge. At low discharge,  $\text{SO}_4$  concentrations are

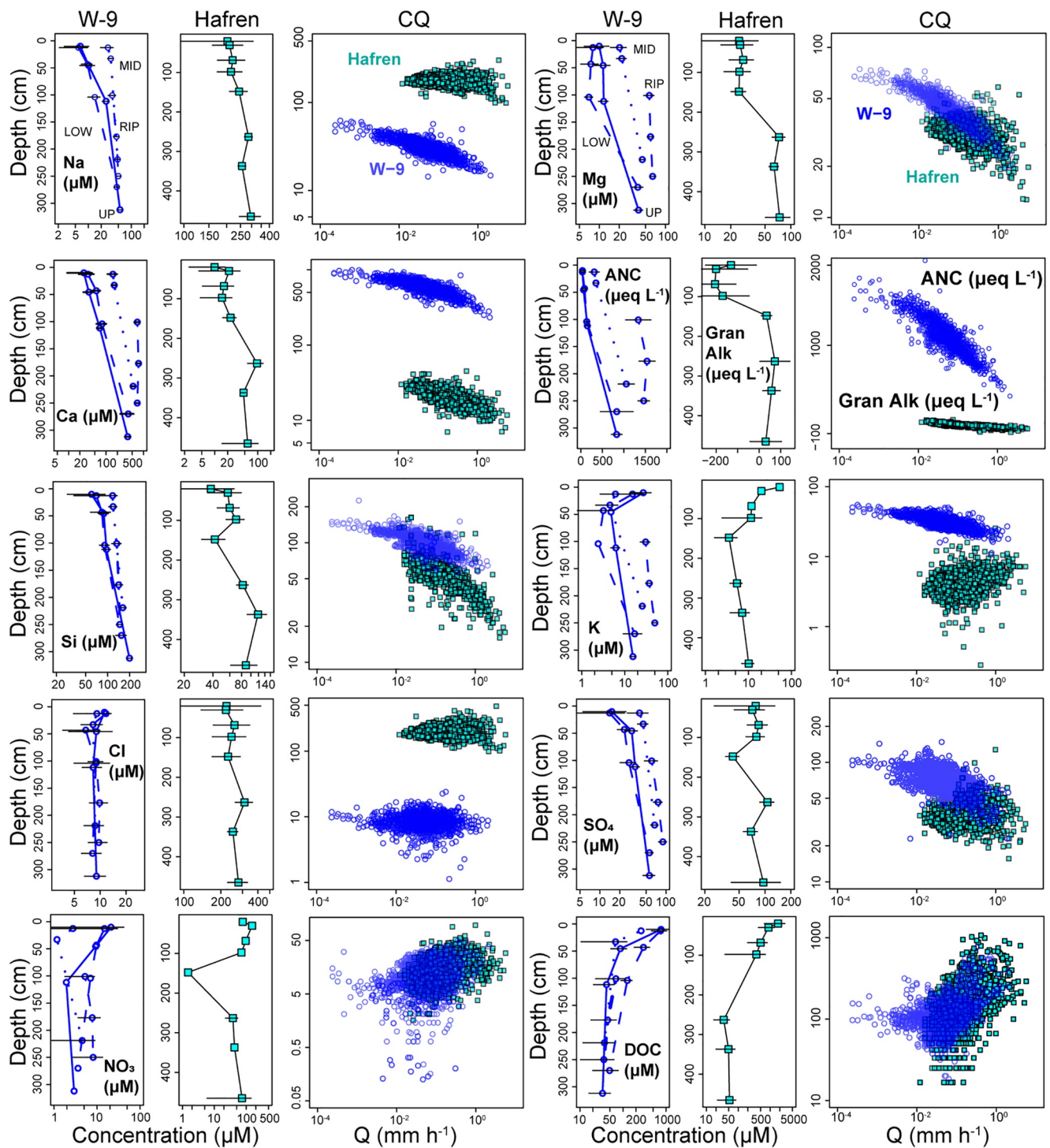


**Figure 5.** Depth profiles and concentration-discharge plots for various solutes at W-9 (blue circles) and Hafren (teal squares). W-9 depth profiles are from multiple locations—hillslope (UP, MID, and LOW positions) and riparian (RIP)—corresponding to soil water and groundwater sampling locations. Hafren depth profiles are averaged from dominant soil types and include data from multiple boreholes (US1, SE3, SE1, and LS4, in order of increasing depth). Error bars in depth profiles are standard deviations of measured concentrations. In general, solutes with higher concentrations in the deep zone show dilution patterns while solutes with higher concentrations in the shallow zone show flushing patterns.

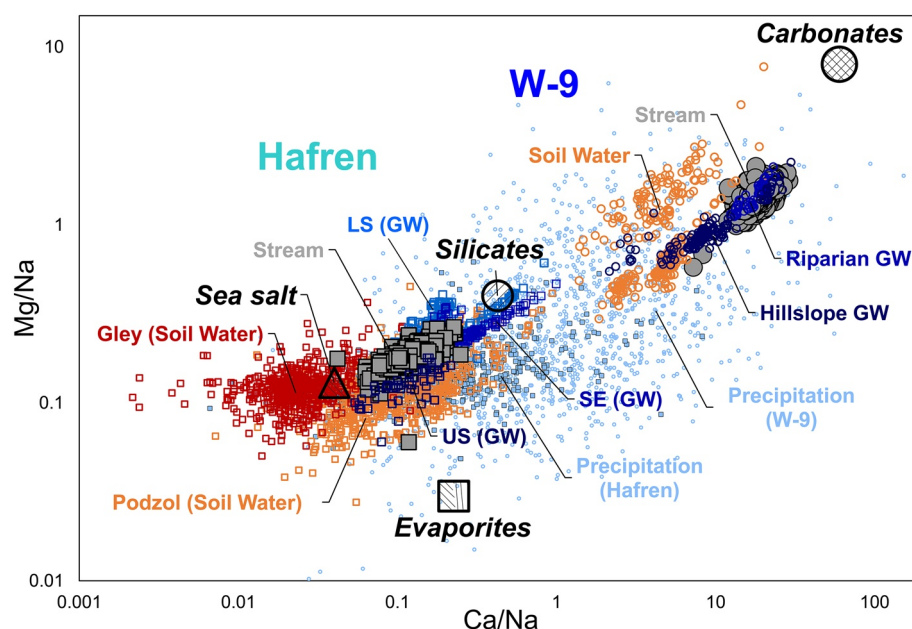


**Figure 6.** Molar ratios for Mg/Na versus Ca/Na in streamwater, soil water, and groundwater at W-9 (right, Ca/Na > 1) and Hafren (left, Ca/Na < 1), along with theoretical ranges for ratios of carbonate, silicate, and evaporite lithologies (Gaillardet et al., 1999) and sea salt (Schlesinger et al., 1982). Groundwater boreholes from Hafren include the Upper Slope as US (GW), Lower Slope as LS (GW), and South East as SE (GW). Streamwater in both sites are a mixture of soil water and groundwater, as indicated along similar molar ratio lines. Precipitation water has large variations and is modified considerably before entering streams. Soil water has a much larger spread in chemical signature than groundwater. Hafren streamwater resembles sea salt and silicate lithology, whereas W-9 resembles carbonate and silicate lithology.

approximately 30–40  $\mu\text{M}$ . As discharge increases, the concentrations vary from 20 to 70  $\mu\text{M}$ . The concentrations of  $\text{SO}_4$  in the shallow soil water range from 70 to 85  $\mu\text{M}$ , while concentrations in groundwater range from 42 to 107  $\mu\text{M}$ , depending on the sampled borehole. In other words, there is no clear increasing or decreasing trend with depth, consistent with the observed CQ pattern with large variation but no clear increasing or decreasing trend.

### 3.3. End Member Analysis

The molar ratios of Mg/Na and Ca/Na in different waters at W-9 and Hafren (Figure 6) depict the range of chemical signatures for different source waters contributing to streamwater and illustrate how solute concentration ratios differ with different lithology. The clustering of different source waters around streamwater indicates which sources could be predominant. The proximity of specific end members to the stream data can be interpreted as reflecting their influence on stream chemistry. At W-9, both groundwater (hillslope and riparian) and streamwater have high Mg/Na and Ca/Na ratios and are more similar to carbonate lithology, indicating their origin from carbonate-dominated rock. The soil water samples generally have lower Ca/Na ratios than the groundwater samples, consistent with the limited carbonate in shallow soils. Some soil water measurements have much higher Mg/Na ratios and deviate from the rest of the W-9 data, suggesting that these sources of soil water do not contribute to the stream. The ratios of hillslope groundwater span a large range, overlapping with the low ratios in soil water and high ratios in riparian groundwater. This overlap suggests interaction between different source waters, as soil water may contribute to hillslope groundwater while hillslope groundwater may contribute to riparian groundwater. At Hafren, the cation ratios in streamwater are close to silicates and sea salt, consistent with the chemistry of silicate-containing sandstone and mudstone bedrock at the site and the high salt input from the ocean. The US, LS, and SE groundwater concentration ratios overlap with the Lower Hafren streamwater, whereas the podzol and gley soil waters both have larger ranges of Ca/Na and Mg/Na ratios than the streamwater. Interestingly, precipitation chemistry spans a wide range of the solute ratio figure and does not resemble stream chemistry or

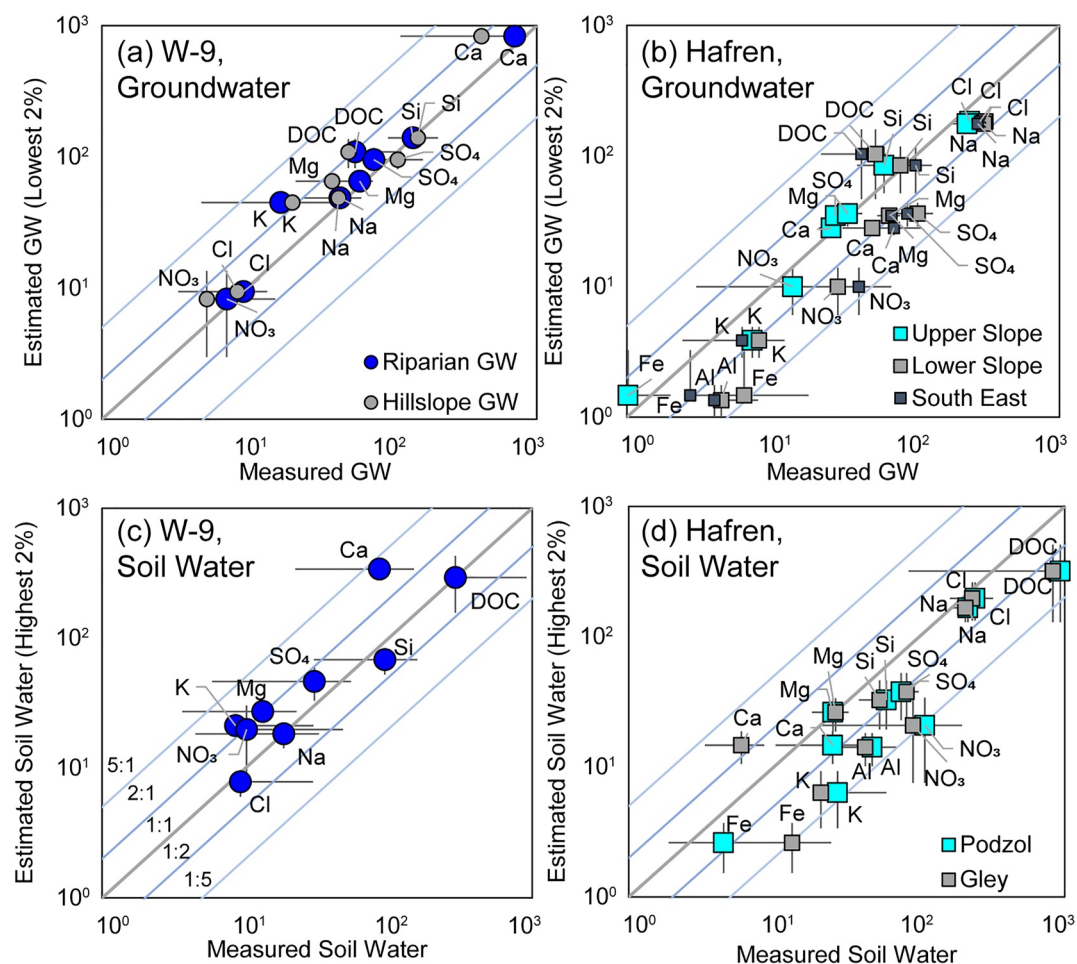


**Figure 7.** Estimated versus measured chemistry (in  $\mu\text{M}$ ) for (a) groundwater at W-9, with measured values for hillslope groundwater and riparian groundwater; and (c) soil water at W-9, with measured values averaged from all lysimeters. Estimated versus measured chemistry for (b) groundwater at Hafren, with measured values for Upper Slope, Lower Slope, and South East boreholes, and (d) soil water at Hafren, with measured values averaged for podzol and gley soils. All estimated values for groundwater are from the lowest 2% of sampled discharge; all estimated values for soil water are from the highest 2% of sampled discharge. Vertical error bars are standard deviations of estimated concentrations. Horizontal error bars are propagated standard deviations of measured groundwater and soil water concentrations (Table S6 in Supporting Information S1). The uncertainty propagation procedure is detailed in Text S2 in Supporting Information S1.

the chemistry of end members. Despite originating from precipitation chemistry, stream chemistry is typically concentrated along molar ratio lines that reflect the chemistry of waters modified by subsurface materials along different flow paths.

### 3.4. Estimated Versus Measured Water Chemistry

Estimated soil water and groundwater concentrations were calculated from the average streamwater concentrations under several cut-off percentages of stream discharge (highest and lowest 1%, 2%, 5%, and 10%). Based on the error analysis (Table S4 in Supporting Information S1), estimates from the highest and lowest 1% and 2% of discharges agreed better with the measured soil water and groundwater concentrations than estimates derived from the highest and lowest 5% and 10% did. This is likely due to the more predominant contribution of soil water at highest flow and groundwater at lowest flow conditions. The estimation errors for the highest and lowest 1% and 2% were not substantially different. We chose to report only the analysis for the highest and lowest 2% as an example.



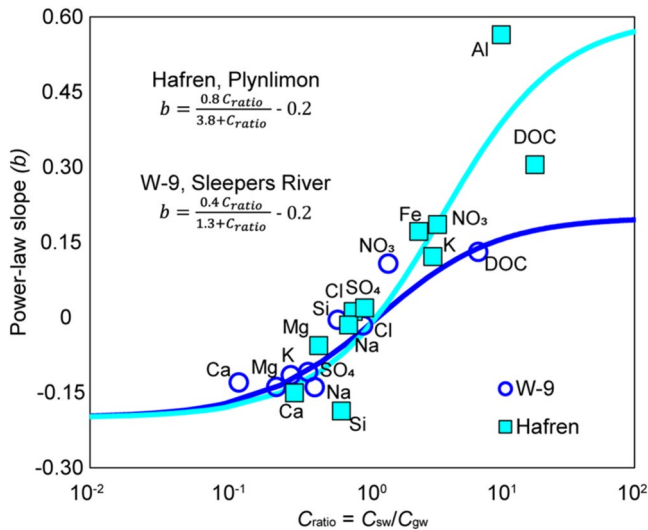


**Figure 8.** Power-law slope ( $b$ ) versus  $C_{ratio}$  ( $= \overline{C_{sw}} / \overline{C_{gw}}$ ) at log scale, where  $\overline{C_{sw}}$  is the average of measured soil water concentrations, and  $\overline{C_{gw}}$  is the average of measured groundwater concentrations. W-9 (open circles): Soil water values averaged from all lysimeters; groundwater values averaged from riparian wells. Hafren (filled squares): Soil water values averaged from podzol and gley soil water data; groundwater values averaged from US, LS, and SE boreholes. At both sites, data points generally follow the equation  $b = \frac{\delta_b C_{ratio}}{C_{ratio}^{\frac{1}{2}} + C_{ratio}} + b_{min}$  proposed in Zhi et al. (2019), although specific parameters differ. This indicates that the shallow and deep water chemistry contrasts  $C_{ratio}$  regulate the CQ power law slope  $b$ .

The relative error was quantified by Equation 5 that compares the estimated to measured concentration ( $\epsilon = \frac{\overline{C_E} - \overline{C_M}}{\overline{C_M}}$ ) (Table S4 in Supporting Information S1). The average  $|\epsilon|$  was used such that negative and positive values did not cancel out to underestimate the average relative error. Measured soil water and groundwater concentrations were compared to corresponding values estimated from stream chemistry at the highest and lowest 2% of sampled discharges (Figure 7). Symbols on the 1:1 line indicate exact agreement between estimated and measured values, whereas deviations from the 1:1 line indicate estimation errors. For example, a point on the 2:1 line means that the concentration was overestimated by a factor of two (i.e.,  $\epsilon = 1$ ). A point on the 1:2 line means that the concentration was underestimated by a factor of two (i.e.,  $\epsilon = -0.5$ ).

The estimated groundwater chemistry at W-9 more closely matched the measured riparian data than the hillslope data (Figure 7a). With the exception of DOC and K, all solutes were estimated within a factor of two for both the riparian and hillslope groundwater (Figure 7a). For riparian groundwater, the average  $|\epsilon|$  value for all solutes was 0.37 ( $\epsilon$ : -0.01 to 1.62; Table S4 in Supporting Information S1). For hillslope groundwater, the average  $|\epsilon|$  value was 0.56 ( $\epsilon$ : -0.13 to 1.19).

At Hafren (Figure 7b), estimated groundwater values matched the US groundwater data better than other boreholes. When compared to the US data,  $\epsilon$  values ranged from -0.48 to 0.44, with an average  $|\epsilon|$  value of 0.27. Estimated values deviated more from the LS groundwater data, with an average  $|\epsilon|$  of 0.55 ( $\epsilon$ : -0.77 and 0.96). Estimated values also deviated appreciably from the SE groundwater data, with an average  $|\epsilon|$  of 0.57 ( $\epsilon$ : -0.75 to 1.45). Propagated standard deviations and coefficients of variation are detailed in Tables S6 and S7 in Supporting Information S1, respectively.

Estimated soil water concentrations at W-9 were mostly within a factor of two of the measured values. The few exceptions were Mg, K, and Ca, which were overestimated with  $\epsilon$  values of 1.06, 1.48, and 2.95, respectively (Figure 7c and Table S4 in Supporting Information S1). The majority of the estimated values at Hafren (Figure 7d) fell below the 1:1 line, indicating a systematic underestimation of soil water concentrations. Most estimated values fell within a factor of three of the measured values, with the exceptions of Fe, Al, K, and  $\text{NO}_3$ , which were underestimated by factors of 3–5. In general, the estimation errors were greater for soil water than for groundwater. The average soil water  $|\epsilon|$  values for all solutes were 0.82 ( $\epsilon$ : -0.27 to 2.95) at W-9, and 0.47 ( $\epsilon$ : -0.81 to 0.03) and 0.57 ( $\epsilon$ : -0.80 to 1.46) for podzol and gley soils at Hafren, respectively.

### 3.5. Power-Law Slope ( $b$ ) Versus $C_{ratio}$ (Shallow and Deep Concentration Ratio)

Following Zhi et al. (2019), we plotted the power-law slope ( $b$ ) of each solute against the  $C_{ratio}$  (Figure 8), the ratio of mean shallow water (soil water) concentration ( $\overline{C_{sw}}$ ) to the mean deeper water (groundwater) concentration ( $\overline{C_{gw}}$ ). This plot shows that  $b$  values mostly increase with shallow versus deep concentration ratios, suggesting that  $C_{ratio}$  shapes export patterns. Data points generally follow the proposed relationship derived from the reactive transport modeling results in Zhi et al. (2019):

$$b = \frac{\delta_b C_{ratio}}{C_{ratio}^{\frac{1}{2}} + C_{ratio}} + b_{min} \quad (6)$$

where  $\delta_b$  is the difference between the maximum ( $b_{max}$ ) and minimum ( $b_{min}$ ) power-law slope of analyzed solutes, and  $C_{ratio,1/2}$  is the concentration ratio corresponding to  $b_{1/2} = \frac{1}{2}(b_{min} + b_{max})$ . The values of  $b_{min}$  are the same between the two sites, while the value of  $\delta_b$  is higher at Hafren than at W-9. At Hafren, several solutes (Si, Al, and DOC) deviate from the curve.

## 4. Discussion

### 4.1. The Shallow and Deep Hypothesis: Linking Flow Paths, Solute Depth Profiles, and Export Patterns

Although recognized in theory, the shallow and deep hypothesis lacks direct data support from collated measurements of soil water, groundwater, and streamwater chemistry. The comprehensive datasets from W-9 and Hafren offer a rare opportunity to directly test the hypothesis and its derivatives: (a) Depth profiles of solute concentrations shape their CQ patterns; (b) Stream chemistry under low- and high-flow conditions can be used to approximate groundwater and soil water chemistry, respectively; (c) CQ power-law slopes ( $b$ ) can be predicted using the shallow-versus-deep concentration ratio ( $C_{ratio}$ ) via Equation 6.

The results support the hypothesis and its derivatives. Comparisons of solute depth profiles and corresponding CQ data show that stream concentrations at low and high discharges approximate the deep and shallow water concentrations in depth profiles, respectively (Figure 5). Concentrations of weathering-derived solutes increase with depth and exhibit dilution patterns in streamwater (e.g., Ca and Mg). Solutes that are abundant in shallow soils have decreasing concentrations with depth, and their CQ plots mostly exhibit flushing patterns (e.g.,  $\text{NO}_3$  and DOC). The CQ power-law slopes ( $b$ ) increase with the shallow versus deep concentration ratios ( $C_{ratio}$ ) (Figure 8) and follow Equation 6, although the specific parameters differ across the two sites.

The alignment of soil water and groundwater chemistry to stream chemistry (Figure 6) suggests their importance as end members to the stream. In contrast, precipitation chemistry spans a much wider range than stream chemistry. Precipitation chemistry is known to be dampened by catchment processing before entering streams, such that both soil water and groundwater chemistry are influenced by precipitation inputs. For example, Cl is primarily derived from atmospheric deposition, but concentrations in the stream are much lower than those in precipitation (Kirchner et al., 2000). Broadly, the hydrology community has known via measurements of streamflow and stable water isotopes that streamwater is mostly “old” water already stored in catchments (Kirchner, 2003, 2019; McDonnell, 1990). Even the “new” water discussed in literature is not the precipitation water itself (Kirchner, 2019), but water less than one week old, or the water traveling to streams via fast flow paths and reemerging with chemistry modified by the subsurface. The direct contribution of precipitation to streamflow is typically minimal unless in short-lived, extremely heavy storm events (Shanley et al., 2002, 2015).

The distinct depth profiles of solutes reflect the interactions among water, soils, roots, microbes, and rocks. In both catchments, the shallow soils are weathered and are enriched in organic materials that act as sources of carbon, nitrogen, and metals, notably Fe and Al (Shand et al., 2005; Shanley, 2000). The deeper subsurface contains reactive minerals such as carbonate (W-9) as well as silicate and pyrite-containing shale (Hafren). In addition, groundwater is typically much older than shallow water, which allows for longer reaction time with parent rocks (Maher, 2011; Torres & Baronas, 2021). In other words, prolonged exposure to parent rocks and longer transit times in groundwater give rise to higher concentrations of weathering-derived solutes at depth and dilution CQ relationships.

Biogenic solutes such as DOC and  $\text{NO}_3$  are produced in shallow soils via processes such as soil respiration and nitrification (Barnes et al., 2018; Jobbágy & Jackson, 2000; Pinay et al., 2015). These solutes can accumulate in shallow soils until large storms flush them into streams (Wen et al., 2020). As DOC and  $\text{NO}_3$  flow deeper into the subsurface, they continue to be used by microbes, such that their concentrations tend to be lower in deeper, older groundwater (Kolbe et al., 2019). Note that the depth distribution of reactive materials observed in the two study sites are common, arising from the nature of weathering and the presence of living things on the Earth's surface and shallow subsurface (Xiao et al., 2021). Therefore, it may be common for weathering-derived solutes to exhibit dilution CQ patterns and biogenic solutes to demonstrate flushing patterns. In fact, multiple large-scale meta-analyses have indicated these widespread CQ patterns. DOC exhibits flushing patterns in more than 90% of sites in the United States (Zarnetske et al., 2018). Most agricultural lands with enriched nitrogen in the shallow soil also exhibit flushing patterns, as shown in catchments worldwide (Botter et al., 2020; Ebeling et al., 2021; Zhi & Li, 2020). Weathering-derived cations have shown both chemostatic (i.e., constant/flat) patterns (Godsey et al., 2009, 2019) and dilution patterns (Zhi et al., 2019). Inorganic carbon quantified as alkalinity or dissolved inorganic carbon often exhibits dilution patterns (Bluth & Kump, 1994; Najjar et al., 2020).

#### 4.2. Reading Subsurface Water Chemistry From Stream Chemistry

If the shallow and deep hypothesis holds, it follows that we can roughly estimate soil water and groundwater chemistry from stream chemistry at high and low flows, respectively (Equations 1–4). Note that the groundwater and soil water concentrations are local measurements, whereas streams drain water from across the entire catchment, integrating spatially heterogeneous and temporally variable chemical signatures of source waters and flow paths (Abbott et al., 2016; McDonnell et al., 2007). Estimation errors are therefore expected: the simple estimation method is meant for first-order approximations of water chemistry closely connected to streams rather than accurate predictions of individual sampling locations across the entire catchment.

As expected, the estimation errors are smaller for riparian groundwater chemistry than for hillslope groundwater chemistry at W-9 (Figure 7), supporting the idea that stream chemistry reflects riparian waters more than hillslope waters (Kiewiet et al., 2019; Musolff et al., 2016; Seibert et al., 2009). Groundwater chemistry can vary significantly at different hillslope locations (Rinderer et al., 2016, 2017). Hillslope waters can become disconnected from streams, especially during summer low flows when they can develop chemistry distinct from that of the stream (McGuire & McDonnell, 2010). Along the flow paths from uphill to streams, water continues to interact with reactive materials, as indicated by lower cation concentrations in hillslope wells compared to riparian wells (Figure 6). Riparian waters therefore integrate the overall reactions along the flow paths. They are also close to the stream and are more likely to directly contribute to and exchange water with the stream.

The larger estimation errors for soil water chemistry could result from large temporal and spatial variations. Acidic atmospheric deposition at W-9 decreased over the several decades when data were collected (Armfield et al., 2019; Shanley et al., 2004). The changing rainfall chemistry in conjunction with complex interactions of critical zone processes (e.g., increased frequency of storm events, breakup of soil aggregates) have been suggested as drivers for increasing stream DOC and a transient legacy of Ca leaching from riparian soils (Adler et al., 2021; Armfield et al., 2019; Cincotta et al., 2019). Hafren also experienced afforestation, deforestation, and acid deposition (Neal et al., 2004, 2010), possibly elevating alkalinity and DOC at the site. In addition, large seasonal and inter-annual variations can lead to variability in decomposition rates of organic carbon and higher concentrations of inorganic carbon and DOC in summers (Laudon et al., 2012). Seasonality also influences processes such as plant uptake, which can drive variations in nutrient availability (Abbott et al., 2018). These temporal variations likely contribute to the challenges in estimating soil water chemistry from stream chemistry.

Spatial heterogeneities introduce another layer of complexity in estimating subsurface water chemistry. Hafren is heterogeneous in terms of vegetation cover, geomorphological features, and bedrock fracture density (Kirchner et al., 2000; Shand et al., 2005). Chemistry between the moorland (Upper Hafren) and forested (Lower Hafren) sub-catchments also differ (Neal et al., 2010). This spatial heterogeneity has led to discrete chemical signatures at different depths and between boreholes (Haria & Shand, 2004; Shand et al., 2005) (Figure 5). W-9 is characterized by significant variations in soil types and organic carbon content (Armfield et al., 2019). Its riparian groundwater has nearly twice the concentration of several solutes (e.g., Ca, K,  $\text{SO}_4$ ,  $\text{NO}_3$ ) as hillslope groundwater (Figure 5). In addition, some sampling locations were fairly distant from the stream gauges (Figure 2), such that the sampled subsurface water may not contribute to streamflow, and the water chemistry in these samples may not be representative of water entering the streams (Hjerdt, 2002; Shanley et al., 2015).

#### 4.3. Beyond the Shallow and Deep Hypothesis

The shallow and deep hypothesis highlights the importance of solute depth profiles and flow paths in shaping solute export patterns (Husic et al., 2019; Musolff et al., 2017; Richardson et al., 2020). It is important to keep in mind that in reality, multiple, continuous flow paths contribute to streams (Xiao et al., 2021). Detailed characterization of subsurface structure and flow paths however are scarcely available (Li et al., 2021). The shallow and deep hypothesis represents a simplified conceptual framework for average shallow and deep flow paths that is more in line with current data availability. More complex frameworks can be formulated by using the shallow and deep hypothesis as a foundation. Considering this simplified representation of subsurface flow paths, the shallow and deep hypothesis can explain relatively monotonic CQ patterns emerging from two predominant end member source waters.

Previous studies have reported non-monotonic behavior for Si (Torres & Baronas, 2021), sediments and nutrients (Underwood et al., 2017), and a variety of other solutes such as metals (Moatar et al., 2017; Zhi et al., 2019). The concentrations of DOC and  $\text{NO}_3$  at the two study sites here decrease with depth and exhibit flushing CQ relationships. They also exhibit some extent of hysteretic behavior (Figure 5). Both DOC and  $\text{NO}_3$  at W-9 have minimum concentrations at intermediate flow regimes rather than at lowest flows. Therefore, although DOC and  $\text{NO}_3$  broadly increase with discharge, the non-monotonic CQ patterns will require a more complex framework that has more than two end members (Burns et al., 2019; Hooper et al., 1990; Knapp et al., 2020).

Complex, non-monotonic CQ patterns can be shaped not only by vertical stratification but also by horizontal variations that determine the contribution of source waters in different landscape positions to streamflow. For example, Herndon et al. (2015) compared the CQ patterns at Shale Hills (Pennsylvania, United States) with those in two of the Plynlimon catchments. They inferred that the opposite CQ patterns for DOC in these catchments arise from different spatial distributions of organic-rich areas and their varying degrees of hydrologic connectivity to the stream. At Shale Hills, organic-rich swales are connected during low-flow conditions, leading to high DOC concentrations; increasing flow connects organic-poor hillslopes to the stream, leading to diluted DOC (Wen et al., 2020). In contrast, at Plynlimon, organic-rich upland peats are only connected at high-flow conditions, leading to flushing behavior (Herndon et al., 2015). Such analyses underscore the importance of horizontal, or landscape, connectivity in shaping export patterns under certain conditions. Given the multiple dimensions (e.g., vertical, horizontal) of flow in catchments, it is possible that different flow paths activated under varying connectivity conditions influence solute export patterns to varying degrees (Wen et al., 2021; Xiao et al., 2019), potentially leading to non-monotonic CQ patterns. To investigate complex CQ behavior, some authors have suggested splitting CQ plots at threshold discharge values and determining separate CQ patterns and underlying mechanisms at different flow regimes (Moatar et al., 2017; Underwood et al., 2017). These could be interesting directions for further analysis to develop a complex and comprehensive conceptual framework.

## 5. Conclusions

This work collated rare datasets of water chemistry from soils, groundwater, and streams from two intensively monitored catchments in Vermont (W-9 at Sleepers River) and Wales (Hafren at Plynlimon), to directly test the shallow and deep hypothesis. The hypothesis states that contrasting solute export patterns originate from distinct chemical signatures of source waters at different depths (i.e., soil water vs. groundwater) (Figures 4–6). Solute depth profiles and CQ data generally support the shallow and deep hypothesis. Solute profiles that have higher concentrations in groundwater generally show dilution patterns in the stream. In contrast, solutes that have higher concentrations in shallow soil water exhibit flushing patterns in the stream (Figure 5). The chemical contrast between these two source waters ( $C_{\text{ratio}}$ ) determines the CQ export patterns (power law slope  $b$ ) (Figure 8). Shallow soil water chemistry could be roughly estimated from stream chemistry observations collected during the highest 1%–2% of discharge, and deep subsurface water (i.e., groundwater from weathered bedrock/glacial till) chemistry could be approximated from stream chemistry at the lowest 1%–2% of discharge (Figure 7). This approach provides a first-order approximation of scarcely measured soil water and groundwater chemistries using more commonly measured stream chemistry. The ability to infer subsurface water chemistry can help with understanding and quantifying the extent and magnitude of soil biogeochemical reactions and chemical weathering at depth. In addition, stream chemistry can also be used to fathom Earth's subsurface response to changing climate and human perturbations. Overall, the shallow and deep hypothesis offers a simple conceptual foundation upon which complex frameworks can be built to understand hydro-biogeochemical processes under diverse climate, land cover, and geology conditions.

## Data Availability Statement

For Sleepers River, the data used in this work are available in the following references: Shanley et al. (2021); Matt et al. (2021); For Plynlimon, the following data and supporting information to assist in the reuse of the data are freely available for non-commercial use under Open Government Licence terms and conditions from the Environmental Data Information Data Centre (EIDC) (<https://eidc.ac.uk/>; Neal et al. (2013), Norris et al. (2017, 2019) Plynlimon research catchment hydrochemistry. NERC Environmental Information Data Centre. <https://catalogue.ceh.ac.uk/documents/0392bf93-62b2-49f7-8c85-10038f22f0c0>). Figure 2b Acknowledgment: Map data owned



by UK Centre for Ecology & Hydrology and available at: <https://catalogue.ceh.ac.uk/documents/ee2eeee5-e456-4e93-87e9-eee97ee149ee> (catchment boundaries), <https://catalogue.ceh.ac.uk/documents/b5c24a80-af3b-48db-91cd-c796ba5ecc36> (river network), and <https://catalogue.ceh.ac.uk/documents/78bb4a32-765e-4ecf-856b-c970179cdf25> (soil parent materials). Figure 3b Acknowledgment: Daily discharge and precipitation data from: UK National River Flow Archive, <https://nrfa.ceh.ac.uk/data/station/info/54091>, accessed 3 December 2020. Daily temperatures were measured at the Carreg Wen Automatic Weather Station and provided by the UK Centre for Ecology and Hydrology.

## Acknowledgments

We acknowledge Editor Georgia Destouni, the Associate Editor, and three anonymous reviewers for their insightful and constructive reviews. We acknowledge the support of this work from NSF funded projects EAR-1724440 and EAR-2012123 and the long-term support of the U.S. Geological Survey (USGS) Land Change Science program for monitoring the Sleepers River Research Watershed. We thank Serena Matt of the USGS for her efforts on the Sleepers River chemistry data release. We acknowledge the UK Centre for Ecology and Hydrology for maintaining and providing access to the data from the Hafren catchment at Plynlimon. The authors declare no conflicts of interest.

## References

- Abbott, B. W., Baranov, V., Mendoza-Lera, C., Nikolakopoulou, M., Harjung, A., Kolbe, T., et al. (2016). Using multi-tracer inference to move beyond single-catchment ecohydrology. *Earth-Science Reviews*, 160, 19–42. <https://doi.org/10.1016/j.earscirev.2016.06.014>
- Abbott, B. W., Moatar, F., Gauthier, O., Fovet, O., Antoine, V., & Ragueneau, O. (2018). Trends and seasonality of river nutrients in agricultural catchments: 18 years of weekly citizen science in France. *The Science of the Total Environment*, 624, 845–858. <https://doi.org/10.1016/j.scitotenv.2017.12.176>
- Adler, T., Underwood, K. L., Rizzo, D. M., Harpold, A., Sterle, G., Li, L., et al. (2021). Drivers of dissolved organic carbon mobilization from forested headwater catchments: A multi scaled approach. *Frontiers in Water*, 3. <https://doi.org/10.3389/frwa.2021.578608>
- Ameli, A. A., Beven, K., Erlandsson, M., Creed, I. F., McDonnell, J. J., & Bishop, K. (2017). Primary weathering rates, water transit times, and concentration-discharge relations: A theoretical analysis for the critical zone. *Water Resources Research*, 53(1), 942–960. <https://doi.org/10.1002/2016wr019448>
- Anderson, S. P., Dietrich, W. E., Torres, R., Montgomery, D. R., & Loague, K. (1997). Concentration-discharge relationships in runoff from a steep, unchanneled catchment. *Water Resources Research*, 33(1), 211–225. <https://doi.org/10.1029/96wr02715>
- Armfield, J. R., Perdrial, J. N., Gagnon, A., Ehrenkranz, J., Perdrial, N., Cincotta, M., et al. (2019). Does stream water composition at sleepers river in Vermont reflect dynamic changes in soils during recovery from acidification? *Frontiers of Earth Science*, 6. <https://doi.org/10.3389/feart.2018.00246>
- Barnes, R. T., Butman, D. E., Wilson, H. F., & Raymond, P. A. (2018). Riverine export of aged carbon driven by flow path depth and residence time. *Environmental Science & Technology*, 52(3), 1028–1035. <https://doi.org/10.1021/acs.est.7b04717>
- Basu, N. B., Rao, P. S. C., Winzeler, H. E., Kumar, S., Owens, P., & Merwade, V. (2010). Parsimonious modeling of hydrologic responses in engineered watersheds: Structural heterogeneity versus functional homogeneity. *Water Resources Research*, 46(4). <https://doi.org/10.1029/2009wr007803>
- Bell, J. P. (2005). *The soil hydrology of the Plynlimon catchments*. Institute of Hydrology.
- Berghuijs, W. R., & Kirchner, J. W. (2017). The relationship between contrasting ages of groundwater and streamflow. *Geophysical Research Letters*, 44(17), 8925–8935. <https://doi.org/10.1002/2017gl074962>
- Bishop, K., Seibert, J., Köhler, S., & Laudon, H. (2004). Resolving the double paradox of rapidly mobilized old water with highly variable responses in runoff chemistry. *Hydrological Processes*, 18(1), 185–189. <https://doi.org/10.1002/hyp.5209>
- Bluth, G. J. S., & Kump, L. R. (1994). Lithologic and climatologic controls of river chemistry. *Geochimica et Cosmochimica Acta*, 58(10), 2341–2359. [https://doi.org/10.1016/0016-7037\(94\)90015-9](https://doi.org/10.1016/0016-7037(94)90015-9)
- Botter, M., Li, L., Hartmann, J., Burlando, P., & Faticchi, S. (2020). Depth of solute generation is a dominant control on concentration-discharge relations. *Water Resources Research*, 56(8). <https://doi.org/10.1029/2019wr026695>
- Boyer, E. W., Hornberger, G. M., Bencala, K. E., & McKnight, D. M. (1997). Response characteristics of DOC flushing in an alpine catchment. *Hydrological Processes*, 11(12), 1635–1647. [https://doi.org/10.1002/\(sici\)1099-1085\(19971015\)11:12<1635::aid-hyp494>3.0.co;2-h](https://doi.org/10.1002/(sici)1099-1085(19971015)11:12<1635::aid-hyp494>3.0.co;2-h)
- Brandt, C., Robinson, M., & Finch, J. W. (2004). Anatomy of a catchment: The relation of physical attributes of the Plynlimon catchments to variations in hydrology and water status. *Hydrology and Earth System Sciences*, 8(3), 345–354. <https://doi.org/10.5194/hess-8-345-2004>
- Brantley, S. L., Goldhaber, M. B., & Ragnarsdottir, K. V. (2007). Crossing disciplines and scales to understand the critical zone. *Elements*, 3(5), 307–314. <https://doi.org/10.2113/gselements.3.5.307>
- Brantley, S. L., Lebedeva, M. I., Balashov, V. N., Singha, K., Sullivan, P. L., & Stinchcomb, G. (2017). Toward a conceptual model relating chemical reaction fronts to water flow paths in hills. *Geomorphology*, 277, 100–117. <https://doi.org/10.1016/j.geomorph.2016.09.027>
- Burns, D. A., Pellerin, B. A., Miller, M. P., Capel, P. D., Tesoriero, A. J., & Duncan, J. M. (2019). Monitoring the riverine pulse: Applying high-frequency nitrate data to advance integrative understanding of biogeochemical and hydrological processes. *Wiley Interdisciplinary Reviews: Water*, 6(4), e1348. <https://doi.org/10.1002/wat2.1348>
- Buttle, J. M. (1994). Isotope hydrograph separations and rapid delivery of pre-event water from drainage basins. *Progress in Physical Geography*, 18(1), 16–41. <https://doi.org/10.1177/030913339401800102>
- Cincotta, M. M., Perdrial, J. N., Shavitz, A., Libenson, A., Landsman-Gerjoi, M., Perdrial, N., et al. (2019). Soil aggregates as a source of dissolved organic carbon to streams: An experimental study on the effect of solution chemistry on water extractable carbon. *Frontiers in Environmental Science*, 7. <https://doi.org/10.3389/feenvs.2019.00172>
- DeKett, R. G., & Long, R. F. (1995). *Order 1 soil mapping project of the W-9 basin in the Sleepers River watershed*. U.S. Department of Agriculture.
- Diamond, J. S., & Cohen, M. J. (2018). Complex patterns of catchment solute-discharge relationships for coastal plain rivers. *Hydrological Processes*, 32(3). <https://doi.org/10.1002/hyp.11424>
- Dunne, T., & Black, R. D. (1971). Runoff processes during snowmelt. *Water Resources Research*, 7(5), 1160–1172. <https://doi.org/10.1029/wr007i005p01160>
- Ebeling, P., Kumar, R., Weber, M., Knoll, L., Fleckenstein, J. H., & Musolff, A. (2021). Archetypes and controls of riverine nutrient export across German catchments. *Water Resources Research*, 57(4). <https://doi.org/10.1029/2020wr028134>
- Evans, C., & Davies, T. D. (1998). Causes of concentration/discharge hysteresis and its potential as a tool for analysis of episode hydrochemistry. *Water Resources Research*, 34(1), 129–137. <https://doi.org/10.1029/97wr01881>
- Frisbee, M. D., Wilson, J. L., Gomez-Velez, J. D., Phillips, F. M., & Campbell, A. R. (2013). Are we missing the tail (and the tale) of residence time distributions in watersheds? *Geophysical Research Letters*, 40(17), 4633–4637. <https://doi.org/10.1002/grl.50895>
- Gaillardet, J., Dupré, B., Louvat, P., & Allègre, C. J. (1999). Global silicate weathering and CO<sub>2</sub> consumption rates deduced from the chemistry of large rivers. *Chemical Geology*, 159(1–4), 3–30. [https://doi.org/10.1016/s0009-2541\(99\)00031-5](https://doi.org/10.1016/s0009-2541(99)00031-5)

- Godsey, S. E., Hartmann, J., & Kirchner, J. W. (2019). Catchment chemostasis revisited: Water quality responds differently to variations in weather and climate. *Hydrological Processes*, 33(24), 3056–3069. <https://doi.org/10.1002/hyp.13554>
- Godsey, S. E., Kirchner, J. W., & Clow, D. W. (2009). Concentration-discharge relationships reflect chemostatic characteristics of US catchments. *Hydrological Processes*, 23(13), 1844–1864. <https://doi.org/10.1002/hyp.7315>
- Haria, A. H., & Shand, P. (2004). Evidence for deep sub-surface flow routing in forested upland Wales: Implications for contaminant transport and stream flow generation. *Hydrology and Earth System Sciences*, 8(3), 334–344. <https://doi.org/10.5194/hess-8-334-2004>
- Herndon, E. M., Dere, A. L., Sullivan, P. L., Norris, D., Reynolds, B., & Brantley, S. L. (2015). Landscape heterogeneity drives contrasting concentration-discharge relationships in shale headwater catchments. *Hydrology and Earth System Sciences*, 19(8), 3333–3347. <https://doi.org/10.5194/hess-19-3333-2015>
- Hjerdt, K. N. (2002). *Deconvoluting the hydrologic response of a small till catchment: Spatial variability of groundwater level and quality in relation to streamflow* (Ph.D. thesis, p. 204). State University of New York College of Environmental Science and Forestry.
- Hoagland, B., Russo, T. A., Gu, X., Hill, L., Kaye, J., Forsythe, B., & Brantley, S. L. (2017). Hyporheic zone influences on concentration-discharge relationships in a headwater sandstone stream. *Water Resources Research*, 53(6), 4643–4667. <https://doi.org/10.1002/2016wr019717>
- Hooper, R. P., Christophersen, N., & Peters, N. E. (1990). Modelling streamwater chemistry as a mixture of soilwater end-members—An application to the Panola Mountain catchment, Georgia, U.S.A. *Journal of Hydrology*, 116(1–4), 321–343. [https://doi.org/10.1016/0022-1694\(90\)90131-g](https://doi.org/10.1016/0022-1694(90)90131-g)
- Husic, A., Fox, J., Adams, E., Ford, W., Agouridis, C., Currans, J., & Backus, J. (2019). Nitrate pathways, processes, and timing in an agricultural Karst system: Development and application of a numerical model. *Water Resources Research*, 55(3), 2079–2103. <https://doi.org/10.1029/2018wr023703>
- Jasechko, S., Kirchner, J. W., Welker, J. M., & McDonnell, J. J. (2016). Substantial proportion of global streamflow less than three months old. *Nature Geoscience*, 9(2), 126–129. <https://doi.org/10.1038/ngeo2636>
- Jin, L., Ravella, R., Ketchum, B., Bierman, P. R., Heaney, P., White, T., & Brantley, S. L. (2010). Mineral weathering and elemental transport during hillslope evolution at the Susquehanna/Shale Hills Critical Zone Observatory. *Geochimica et Cosmochimica Acta*, 74(13), 3669–3691. <https://doi.org/10.1016/j.gca.2010.03.036>
- Jobbágy, E. G., & Jackson, R. B. (2000). The vertical distribution of soil organic carbon and its relation to climate and vegetation. *Ecological Applications*, 10(2), 423–436. [https://doi.org/10.1890/1051-0761\(2000\)010\[0423:tvdsos\]2.0.co;2](https://doi.org/10.1890/1051-0761(2000)010[0423:tvdsos]2.0.co;2)
- Johnson, N. M., Likens, G. E., Bormann, F. H., Fisher, D. W., & Pierce, R. S. (1969). A working model for the variation in stream water chemistry at the Hubbard Brook experimental forest, New Hampshire. *Water Resources Research*, 5(6), 1353–1363. <https://doi.org/10.1029/wr005i006p01353>
- Kendall, K. A., Shanley, J. B., & McDonnell, J. J. (1999). A hydrometric and geochemical approach to test the transmissivity feedback hypothesis during snowmelt. *Journal of Hydrology*, 219(3–4), 188–205. [https://doi.org/10.1016/s0022-1694\(99\)00059-1](https://doi.org/10.1016/s0022-1694(99)00059-1)
- Kiewiet, L., von Freyberg, J., & van Meerveld, H. J. (2019). Spatiotemporal variability in hydrochemistry of shallow groundwater in a small pre-alpine catchment: The importance of landscape elements. *Hydrological Processes*, 33(19), 2502–2522. <https://doi.org/10.1002/hyp.13517>
- Kirby, C., Newson, M. D., & Gilman, K. (1991). *Plynlimon research: The first two decades* (Vol. 109).
- Kirchner, J. W. (2003). A double paradox in catchment hydrology and geochemistry. *Hydrological Processes*, 17(4), 871–874. <https://doi.org/10.1002/hyp.5108>
- Kirchner, J. W. (2019). Quantifying new water fractions and transit time distributions using ensemble hydrograph separation: Theory and benchmark tests. *Hydrology and Earth System Sciences*, 23(1), 303–349. <https://doi.org/10.5194/hess-23-303-2019>
- Kirchner, J. W., Feng, X., & Neal, C. (2000). Fractal stream chemistry and its implications for contaminant transport in catchments. *Nature*, 403(6769), 524–527. <https://doi.org/10.1038/35000537>
- Kirchner, J. W., Feng, X., & Neal, C. (2001). Catchment-scale advection and dispersion as a mechanism for fractal scaling in stream tracer concentrations. *Journal of Hydrology*, 254, 82–101. [https://doi.org/10.1016/s0022-1694\(01\)00487-5](https://doi.org/10.1016/s0022-1694(01)00487-5)
- Kirchner, J. W., & Neal, C. (2013). Universal fractal scaling in stream chemistry and its implications for solute transport and water quality trend detection. *Proceedings of the National Academy of Sciences of the United States of America*, 110(30), 12213–12218. <https://doi.org/10.1073/pnas.1304328110>
- Klaus, J., & McDonnell, J. J. (2013). Hydrograph separation using stable isotopes: Review and evaluation. *Journal of Hydrology*, 505, 47–64. <https://doi.org/10.1016/j.jhydrol.2013.09.006>
- Knapp, J. L. A., Neal, C., Schlumpf, A., Neal, M., & Kirchner, J. W. (2019). New water fractions and transit time distributions at Plynlimon, Wales, estimated from stable water isotopes in precipitation and streamflow. *Hydrology and Earth System Sciences*, 23(10), 4367–4388. <https://doi.org/10.5194/hess-23-4367-2019>
- Knapp, J. L. A., von Freyberg, J., Studer, B., Kiewiet, L., & Kirchner, J. W. (2020). Concentration-discharge relationships vary among hydrological events, reflecting differences in event characteristics. *Hydrology and Earth System Sciences*, 24(5), 2561–2576. <https://doi.org/10.5194/hess-24-2561-2020>
- Kolbe, T., de Dreuzy, J.-R., Abbott, B. W., Aquilina, L., Babey, T., Green, C. T., et al. (2019). Stratification of reactivity determines nitrate removal in groundwater. *Proceedings of the National Academy of Sciences*, 116(7), 2494–2499. <https://doi.org/10.1073/pnas.1816892116>
- Laudon, H., Buttle, J., Carey, S. K., McDonnell, J., McGuire, K., Seibert, J., et al. (2012). Cross-regional prediction of long-term trajectory of stream water DOC response to climate change. *Geophysical Research Letters*, 39(18). <https://doi.org/10.1029/2012gl053033>
- Laudon, H., Seibert, J., Köhler, S., & Bishop, K. (2004). Hydrological flow paths during snowmelt: Congruence between hydrometric measurements and oxygen 18 in meltwater, soil water, and runoff. *Water Resources Research*, 40(3). <https://doi.org/10.1029/2003wr002455>
- Li, L., Maher, K., Navarre-Sitchler, A., Druhan, J., Meile, C., Lawrence, C., et al. (2017). Expanding the role of reactive transport models in critical zone processes. *Earth-Science Reviews*, 165, 280–301. <https://doi.org/10.1016/j.earscirev.2016.09.001>
- Li, L., Sullivan, P. L., Benettin, P., Cirpka, O. A., Bishop, K., Brantley, S. L., et al. (2021). Toward catchment hydro-biogeochemical theories. *Wiley Interdisciplinary Reviews: Water*, 8(1). <https://doi.org/10.1002/wat2.1495>
- Maher, K. (2011). The role of fluid residence time and topographic scales in determining chemical fluxes from landscapes. *Earth and Planetary Science Letters*, 312(1–2), 48–58. <https://doi.org/10.1016/j.epsl.2011.09.040>
- Matt, S., Shanley, J. B., Chalmers, A. T., Sebestyen, S. D., Merriam, J., Bailey, S. W., et al. (2021). *Water chemistry database, Sleepers River research watershed, Danville, Vermont, 1991–2018*. U.S. Geological Survey data release. <https://doi.org/10.5066/P9380HQG>
- McDonnell, J. J. (1990). A Rationale for old water discharge through macropores in a steep, humid catchment. *Water Resources Research*, 26(11), 2821–2832. <https://doi.org/10.1029/wr026i011p02821>
- McDonnell, J. J., Sivapalan, M., Vache, K., Dunn, S., Grant, G., Haggerty, R., et al. (2007). Moving beyond heterogeneity and process complexity: A new vision for watershed hydrology. *Water Resources Research*, 43(7). <https://doi.org/10.1029/2006wr005467>
- McGlynn, B. L., McDonnell, J. J., & Branner, D. D. (2002). A review of the evolving perceptual model of hillslope flowpaths at the Maimai catchments, New Zealand. *Journal of Hydrology*, 257(1), 1–26. [https://doi.org/10.1016/s0022-1694\(01\)00559-5](https://doi.org/10.1016/s0022-1694(01)00559-5)

- McGlynn, B. L., McDonnell, J. J., Shanley, J. B., & Kendall, C. (1999). Riparian zone flowpath dynamics during snowmelt in a small headwater catchment. *Journal of Hydrology*, 222(1–4), 75–92. [https://doi.org/10.1016/S0022-1694\(99\)00102-X](https://doi.org/10.1016/S0022-1694(99)00102-X)
- McGuire, K. J., & McDonnell, J. J. (2010). Hydrological connectivity of hillslopes and streams: Characteristic time scales and nonlinearities. *Water Resources Research*, 46(10). <https://doi.org/10.1029/2010WR009341>
- McIntosh, J. C., Schaumburg, C., Perdrial, J., Harpold, A., Vázquez-Ortega, A., Rasmussen, C., et al. (2017). Geochemical evolution of the critical zone across variable time scales informs concentration-discharge relationships: Jemez river basin critical zone observatory. *Water Resources Research*, 53(3), 4169–4196. <https://doi.org/10.1002/2016WR019712>
- Moatar, F., Abbott, B. W., Minaudo, C., Curie, F., & Pinay, G. (2017). Elemental properties, hydrology, and biology interact to shape concentration-discharge curves for carbon, nutrients, sediment, and major ions. *Water Resources Research*, 53(2), 1270–1287. <https://doi.org/10.1002/2016wr019635>
- Mulholland, P. J. (1993). Hydrometric and stream chemistry evidence of three storm flowpaths in walker branch watershed. *Journal of Hydrology*, 151(2), 291–316. [https://doi.org/10.1016/0022-1694\(93\)90240-A](https://doi.org/10.1016/0022-1694(93)90240-A)
- Musolff, A., Fleckenstein, J. H., Rao, P. S. C., & Jawitz, J. W. (2017). Emergent archetype patterns of coupled hydrologic and biogeochemical responses in catchments. *Geophysical Research Letters*, 44(9), 4143–4151. <https://doi.org/10.1002/2017gl072630>
- Musolff, A., Schmidt, C., Rode, M., Lischeid, G., Weise, S. M., & Fleckenstein, J. H. (2016). Groundwater head controls nitrate export from an agricultural lowland catchment. *Advances in Water Resources*, 96, 95–107. <https://doi.org/10.1016/j.advwatres.2016.07.003>
- Musolff, A., Schmidt, C., Selle, B., & Fleckenstein, J. H. (2015). Catchment controls on solute export. *Advances in Water Resources*, 86, 133–146. <https://doi.org/10.1016/j.advwatres.2015.09.026>
- Najjar, R. G., Herrmann, M., Cintrón Del Valle, S. M., Friedman, J. R., Friedrichs, M. A. M., Harris, L. A., et al. (2020). Alkalinity in tidal tributaries of the Chesapeake Bay. *Journal of Geophysical Research: Oceans*, 125(1). <https://doi.org/10.46427/gold2020.1885>
- Neal, C., Kirchner, J., & Reynolds, B. (2013). *Plynlimon research catchment hydrochemistry*. NERC Environmental Information Data Centre. <https://doi.org/10.5285/44095e17-43b0-45d4-a781-aab4f72da025>
- Neal, C., & Kirchner, J. W. (2000). Sodium and chloride levels in rainfall, mist, streamwater and groundwater at the Plynlimon catchments, mid-Wales: Inferences on hydrological and chemical controls. *Hydrology and Earth System Sciences*, 4(2), 295–310. <https://doi.org/10.5194/hess-4-295-2000>
- Neal, C., Reynolds, B., Neal, M., Wickham, H., Hill, L., & Williams, B. (2004). The impact of conifer harvesting on stream water quality: The Afon Hafren, mid-Wales. *Hydrology and Earth System Sciences*, 8(3), 503–520. <https://doi.org/10.5194/hess-8-503-2004>
- Neal, C., Reynolds, B., Rowland, P., Norris, D., Kirchner, J. W., Neal, M., et al. (2012). High-frequency water quality time series in precipitation and streamflow: From fragmentary signals to scientific challenge. *The Science of the Total Environment*, 434, 3–12. <https://doi.org/10.1016/j.scitotenv.2011.10.072>
- Neal, C., Robinson, M., Reynolds, B., Neal, M., Rowland, P., Grant, S., et al. (2010). Hydrology and water quality of the headwaters of the River Severn: Stream acidity recovery and interactions with plantation forestry under an improving pollution climate. *The Science of the Total Environment*, 408(21), 5035–5051. <https://doi.org/10.1016/j.scitotenv.2010.07.047>
- Neal, C., & Rosier, P. T. W. (1990). Chemical studies of chloride and stable oxygen isotopes in two conifer afforested and moorland sites in the British uplands. *Journal of Hydrology*, 115, 269–283. [https://doi.org/10.1016/0022-1694\(90\)90209-g](https://doi.org/10.1016/0022-1694(90)90209-g)
- Neal, C., Smith, C. J., Walls, J., Billingham, P., Hill, S., & Neal, M. (1990). Hydrogeochemical variations in Hafren forest stream waters, mid-Wales. *Journal of Hydrology*, 116, 185–200. [https://doi.org/10.1016/0022-1694\(90\)90122-e](https://doi.org/10.1016/0022-1694(90)90122-e)
- Norris, D. A., Harvey, R., Winterbourn, J. M., Hughes, S., Lebron, I., Thacker, S. A., et al. (2017). *Plynlimon research catchment hydrochemistry (2011–2016)*. NERC Environmental Information Data Centre. <https://doi.org/10.5285/794c609b-da62-4a42-a4c1-267219865bb1>
- Norris, D. A., Harvey, R., Winterbourn, J. M., Lebron, I., Thacker, S. A., Lawlor, A. J., et al. (2019). *Plynlimon research catchment hydrochemistry (2011–2016)*. NERC Environmental Information Data Centre. <https://doi.org/10.5285/54fe47f3-778e-4e0b-8cf5-b2fda2473b7f>
- Pacific, V. J., Jencso, K. G., & McGlynn, B. L. (2010). Variable flushing mechanisms and landscape structure control stream DOC export during snowmelt in a set of nested catchments. *Biogeochemistry*, 99(1–3), 193–211. <https://doi.org/10.1007/s10533-009-9401-1>
- Pinay, G., Peiffer, S., De Dreuzy, J.-R., Krause, S., Hannah, D. M., Fleckenstein, J. H., et al. (2015). Upscaling nitrogen removal capacity from local hotspots to low stream orders' drainage basins. *Ecosystems*, 18(6), 1101–1120. <https://doi.org/10.1007/s10021-015-9878-5>
- Pinder, G. F., & Jones, J. F. (1969). Determination of the ground-water component of peak discharge from the chemistry of total runoff. *Water Resources Research*, 5(2), 438–445. <https://doi.org/10.1029/wr005i002p00438>
- Reynolds, B., Fowler, D., Smith, R. I., & Hall, J. R. (1997). Atmospheric inputs and catchment solute fluxes for major ions in five Welsh upland catchments. *Journal of Hydrology*, 194, 305–329. [https://doi.org/10.1016/S0022-1694\(96\)03226-X](https://doi.org/10.1016/S0022-1694(96)03226-X)
- Reynolds, B., Neal, C., Hornung, M., Hughes, S., & Stevens, P. A. (1988). Impact of afforestation on the soil solution chemistry of Stagnopodzols in mid-Wales. *Water, Air, & Soil Pollution*, 38, 55–70. <https://doi.org/10.1007/bf00279585>
- Richardson, C. M., Zimmer, M. A., Fackrell, J. K., & Paytan, A. (2020). Geologic controls on source water drive baseflow generation and carbon geochemistry: Evidence of nonstationary baseflow sources across multiple subwatersheds. *Water Resources Research*, 56(7), e2019WR026577. <https://doi.org/10.1029/2019wr026577>
- Riebe, C. S., Hahm, W. J., & Brantley, S. L. (2017). Controls on deep critical zone architecture: A historical review and four testable hypotheses. *Earth Surface Processes and Landforms*, 42(1), 128–156. <https://doi.org/10.1002/esp.4052>
- Rinderer, M., McGlynn, B. L., & van Meerveld, H. J. (2017). Groundwater similarity across a watershed derived from time-warped and flow-corrected time series. *Water Resources Research*, 53(5), 3921–3940. <https://doi.org/10.1002/2016wr019856>
- Rinderer, M., van Meerveld, I., Stähli, M., & Seibert, J. (2016). Is groundwater response timing in a pre-alpine catchment controlled more by topography or by rainfall? *Hydrological Processes*, 30(7), 1036–1051. <https://doi.org/10.1002/hyp.10634>
- Schlesinger, W. H., Gray, J. T., & Gilliam, F. S. (1982). Atmospheric deposition processes and their importance as sources of nutrients in a Chaparral Ecosystem of Southern California. *Water Resources Research*, 18, 623–629. <https://doi.org/10.1029/wr018i003p00623>
- Searcy, J. K. (1959). *Flow-duration curves: Manual of hydrology: Part 2: Low-flow techniques*. US. Gov. Pr. Office.
- Seibert, J., Grabs, T., Köhler, S., Laudon, H., Winterdahl, M., & Bishop, K. (2009). Linking soil- and stream-water chemistry based on a Riparian flow-concentration integration model. *Hydrology and Earth System Sciences*, 13(12), 2287–2297. <https://doi.org/10.5194/hess-13-2287-2009>
- Shand, P., Darbyshire, D. P. F., Gooddy, D., & Haria, A. H. (2007).  $^{87}\text{Sr}/^{86}\text{Sr}$  as an indicator of flowpaths and weathering rates in the Plynlimon experimental catchments, Wales, U.K. *Chemical Geology*, 236(3–4), 247–265. <https://doi.org/10.1016/j.chemgeo.2006.09.012>
- Shand, P., Haria, A. H., Neal, C., Griffiths, K. J., Gooddy, D. C., Dixon, A. J., et al. (2005). Hydrochemical heterogeneity in an upland catchment: Further characterisation of the spatial, temporal and depth variations in soils, streams and groundwaters of the Plynlimon forested catchment, Wales. *Hydrology and Earth System Sciences*, 9(6), 621–644. <https://doi.org/10.5194/hess-9-621-2005>
- Shanley, J. B. (2000). *Sleepers River, Vermont: A water, energy, and biogeochemical budgets program site* (Rep. Fact Sheet-166-99).



- Shanley, J. B., Chalmers, A. T., Denner, J. C., & Clark, S. F. (2021). *Five-minute discharge, daily precipitation, stream runoff, and maximum and minimum air temperature; and annual precipitation and runoff for W-9 catchment, Sleepers River Research Watershed near Danville, Vermont, 1991–2018*. U.S. Geological Survey data release. <https://doi.org/10.5066/P929KMVK>
- Shanley, J. B., Kendall, C., Smith, T. E., Wolock, D. M., & McDonnell, J. J. (2002). Controls on old and new water contributions to stream flow at some nested catchments in Vermont, USA. *Hydrological Processes*, 16(3), 589–609. <https://doi.org/10.1002/hyp.312>
- Shanley, J. B., Krám, P., Hruška, J., & Bullen, T. D. (2004). A biogeochemical comparison of two well-buffered catchments with contrasting histories of acid deposition. *Water, Air, and Soil Pollution: Focus*, 4(2/3), 325–342. <https://doi.org/10.1023/b:wafa.0000028363.48348.a4>
- Shanley, J. B., Sebestyen, S. D., McDonnell, J. J., McGlynn, B. L., & Dunne, T. (2015). Water's way at Sleepers River watershed—Revisiting flow generation in a post-glacial landscape, Vermont USA. *Hydrological Processes*, 29(16), 3447–3459. <https://doi.org/10.1002/hyp.10377>
- Shanley, J. B., Sebestyen, S. D., Smith, T. E., Chalmers, A. T., Clark, S. F., & Denner, J. C. (2019). Groundwater level data for Watershed-9 (W-9) in the Sleepers River Research Watershed (Vermont). Forest Service Research Data Archive. <https://doi.org/10.2737/RDS-2018-0064>
- Stevens, P. A., Reynolds, B., Hughes, S., Norris, D. A., & Dickinson, A. L. (1997). Relationships between spruce plantation age, solute and soil chemistry in Hafren forest. *Hydrology and Earth System Sciences*, 1(3), 627–637. <https://doi.org/10.5194/hess-1-627-1997>
- Sullivan, P. L., Hynek, S. A., Gu, X., Singha, K., White, T., West, N., et al. (2016). Oxidative dissolution under the channel leads geomorphological evolution at the Shale Hills catchment. *American Journal of Science*, 316(10), 981–1026. <https://doi.org/10.2475/10.2016.02>
- Swistock, B. R., Yamon, J. J., Dewalle, D. R., & Sharpe, W. E. (1990). Comparison of soil water chemistry and sample size requirements for Pan vs Tension lysimeters. *Water, Air, & Soil Pollution*, 50, 387–396. <https://doi.org/10.1007/bf00280637>
- Tallaksen, L. M. (1995). A review of baseflow recession analysis. *Journal of Hydrology*, 165(1), 349–370. [https://doi.org/10.1016/0022-1694\(94\)02540-r](https://doi.org/10.1016/0022-1694(94)02540-r)
- Thompson, S. E., Basu, N. B., Lascrain, J., Aubeneau, A., & Rao, P. S. C. (2011). Relative dominance of hydrologic versus biogeochemical factors on solute export across impact gradients. *Water Resources Research*, 47(10). <https://doi.org/10.1029/2010wr009605>
- Torres, M. A., & Baronas, J. J. (2021). Modulation of riverine concentration-discharge relationships by changes in the shape of the water transit time distribution. *Global Biogeochemical Cycles*, 35(1). <https://doi.org/10.1029/2020gb006694>
- Torres, M. A., West, A. J., & Clark, K. E. (2015). Geomorphic regime modulates hydrologic control of chemical weathering in the Andes–Amazon. *Geochimica et Cosmochimica Acta*, 166, 105–128. <https://doi.org/10.1016/j.gca.2015.06.007>
- Underwood, K. L., Rizzo, D. M., Schroth, A. W., & Dewoolkar, M. M. (2017). Evaluating spatial variability in sediment and phosphorus concentration-discharge relationships using bayesian inference and self-organizing maps. *Water Resources Research*, 53(12), 10293–10316. <https://doi.org/10.1002/2017wr021353>
- Welch, L. A., & Allen, D. M. (2014). Hydraulic conductivity characteristics in mountains and implications for conceptualizing bedrock groundwater flow. *Hydrogeology Journal*, 22(5), 1003–1026. <https://doi.org/10.1007/s10040-014-1121-5>
- Wen, H., Brantley, S. L., Davis, K. J., Duncan, J. M., & Li, L. (2021). The limits of homogenization: What hydrological dynamics can a simple model represent at the catchment scale? *Water Resources Research*, 57(6). <https://doi.org/10.1029/2020wr029528>
- Wen, H., & Li, L. (2018). An upscaled rate law for mineral dissolution in heterogeneous media: The role of time and length scales. *Geochimica et Cosmochimica Acta*, 235, 1–20. <https://doi.org/10.1016/j.gca.2018.04.024>
- Wen, H., Perdrial, J., Abbott, B. W., Bernal, S., Dupas, R., Godsey, S. E., et al. (2020). Temperature controls production but hydrology regulates export of dissolved organic carbon at the catchment scale. *Hydrology and Earth System Sciences*, 24(2), 945–966. <https://doi.org/10.5194/hess-24-945-2020>
- Wittenberg, H. (1999). Baseflow recession and recharge as nonlinear storage processes. *Hydrological Processes*, 13(5), 715–726. [https://doi.org/10.1002/\(sici\)1099-1085\(19990415\)13:5<715::aid-hyp775>3.0.co;2-n](https://doi.org/10.1002/(sici)1099-1085(19990415)13:5<715::aid-hyp775>3.0.co;2-n)
- Worrall, F., Burt, T. P., & Adamson, J. (2008). Long-term records of dissolved organic carbon flux from peat-covered catchments: Evidence for a drought effect? *Hydrological Processes*, 22(16), 3181–3193. <https://doi.org/10.1002/hyp.6907>
- Xiao, D., Brantley, S. L., & Li, L. (2021). Vertical connectivity regulates water transit time and chemical weathering at the hillslope scale. *Water Resources Research*, 57(8). <https://doi.org/10.1029/2020wr029207>
- Xiao, D., Shi, Y., Brantley, S. L., Forsythe, B., DiBiase, R., Davis, K., & Li, L. (2019). Streamflow generation from catchments of contrasting lithologies: The role of soil properties, topography, and catchment size. *Water Resources Research*, 55(11), 9234–9257. <https://doi.org/10.1029/2018wr023736>
- Zarnetske, J. P., Bouda, M., Abbott, B. W., Saiers, J., & Raymond, P. A. (2018). Generality of hydrologic transport limitation of watershed organic carbon flux across ecoregions of the United States. *Geophysical Research Letters*, 45(21), 11,702–11,711. <https://doi.org/10.1029/2018gl080005>
- Zhi, W., & Li, L. (2020). The shallow and deep hypothesis: Subsurface vertical chemical contrasts shape nitrate export patterns from different land uses. *Environmental Science & Technology*, 54(19), 11915–11928. <https://doi.org/10.1021/acs.est.0c01340>
- Zhi, W., Li, L., Dong, W., Brown, W., Kaye, J., Steefel, C., & Williams, K. H. (2019). Distinct source water chemistry shapes contrasting concentration-discharge patterns. *Water Resources Research*, 55(5), 4233–4251. <https://doi.org/10.1029/2018wr024257>

## Reference From the Supporting Information

- Musolf, A., Fleckenstein, J. H., Rao, P. S. C., & Jawitz, J. W. (2017). Emergent archetype patterns of coupled hydrologic and biogeochemical responses in catchments. *Geophysical Research Letters*, 44(9), 4143–4151.